^{195}Pt NMR—theory and application

Brett M. Still, P. G. Anil Kumar, Janice R. Aldrich-Wright and William S. Price*

Received 2nd May 2006
First published as an Advance Article on the web 17th November 2006
DOI: 10.1039/b606190g

This *critical review* highlights the progress in ^{195}Pt NMR over the last 25 years. In particular, some of the recent applications of ^{195}Pt NMR in catalytic and mechanistic studies, intermetallics and drug binding studies are discussed. ^{195}Pt NMR chemical shifts obtained from both theoretical studies and experiments are presented for Pt(0), Pt(II), Pt(III) and Pt(IV) complexes. ^{195}Pt coupling with various nuclei (*viz*. coupling constants) have also been collected in addition to data on ^{195}Pt relaxation. The latest developments in the theoretical knowledge and experimental advances have made ^{195}Pt NMR into a rich source of information in many fields. (164 references.)

1. Introduction

^{195}Pt is the only nuclear magnetic resonance (NMR) active isotope of platinum and it has favourable properties for use in NMR (spin quantum number, $I = ½$, gyromagnetic ratio $\gamma^{195}\text{Pt} = 5.768 \times 10^7$ rad s^{-1} T^{-1}; Larmor frequency 64.5 MHz at 7.05 T, natural abundance 33.8%, relative sensitivity 0.00994 (^{1}H: 1.00), absolute sensitivity 0.00336). Studies involving ^{195}Pt NMR are numerous and date from the 1960s when the sensitivity of the platinum chemical shift (δ^{195}Pt) to structural change was first realised.[1,2] δ^{195}Pt is readily observable and is particularly sensitive to changes in the metal oxidation state, ligand substitution and stereochemistry around the ^{195}Pt nucleus. Due to the prodigious technical and theoretical advances in the last 30 years, NMR spectroscopy is now the technique of choice for structural characterisation of molecules in solution. Among the measurable parameters, chemical shifts are particularly sensitive to molecular composition, conformation, environment and temperature. It has been found that the range of values for δ^{195}Pt span 13 000 ppm and a change of 100 ppm or more is observed when varying ligand substituents.[3] ^{195}Pt NMR is now used in a wide variety of applications including structural elucidation, relaxation studies, kinetics and mechanistic studies and drug binding studies.[4–10] Recently there has been much interest in developing more efficient methods for studying drug binding.[11] Traditionally binding has been measured by observing changes in chemical shifts and intensities of peaks during a time course of 1D ^{195}Pt NMR experiments.[7] A new technique, however, ^{195}Pt Pulsed Gradient Spin-Echo (PGSE) NMR diffusion measurements, has shown promise.[12]

This review will update the field of ^{195}Pt NMR since the last major review in 1982[3] with emphasis on applications, especially to kinetic and mechanistic studies, intermetallics and drug-binding studies. Section 2 is a short introduction to experimental ^{195}Pt NMR methods. Section 3 and Section 4

Nanoscale Organisation and Dynamics Group, College of Health and Science, University of Western Sydney, Penrith South DC, NSW, 1797, Australia. E-mail: w.price@uws.edu.au; Tel: +61-02-4620-3336

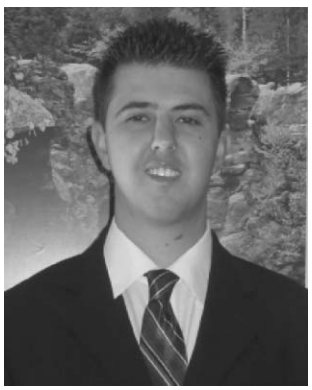

Brett M. Still

Brett M. Still was born in Sydney Australia in 1984. He received his BSc (Honours) from the University of Western Sydney in 2005 and was awarded the University Medal for outstanding candidature. He is now in the first year of his PhD at the same institute under Prof. William S. Price, Assoc. Prof. Janice R. Aldrich-Wright and Assoc. Prof. Frank H. Stootman. His PhD Project involves the development of new methods of NMR diffusion to study drug binding and developing new theoretical models to describe the binding phenomena, especially in relation to chemotherapeutic drugs. He has an interest in classical and quantum mechanics, astronomy and astrophysics. He has a passion for television cartoon series and enjoys, among many sports, tennis and skiing.

Anil Kumar P.G.

Anil Kumar P.G. was born in 1977 in Chickmagalur, India. He received his MSc (Inorganic Chemistry) from Bangalore University in 1999. After a short stint as a research assistant in Indian Institute of Science, Bangalore, he moved to ETH Zürich, Switzerland, to undertake his PhD (2002–2005) under the supervision of Prof. Paul S Pregosin. He is currently working as a post-doctoral research fellow under Prof. William S Price, University of Western Sydney, Australia. He has published 20 research articles on the aspects of transition metal chemistry and NMR. His present research interests involve using multi-dimensional NMR and PGSE diffusion NMR techniques to study platinum anti-cancer drugs; their interaction with proteins and the development of theoretical models studying protein aggregation.

discuss both the theoretical and practical aspects of the chemical shifts and nuclear spin–spin coupling constants (J), respectively. It is difficult to separate the discussion of coupling constants from chemical shifts and so some of the examples are integrated. Significant contributions, however, are highlighted in the appropriate sections. Section 5 deals with the relaxation aspects of ^{195}Pt nuclei. Some of the applications of ^{195}Pt NMR in catalysis and mechanistic studies, intermetallics and drug binding studies are presented in Section 6. A discussion on more advanced NMR techniques is given in Section 7 followed by some closing remarks and future prospects of ^{195}Pt NMR in Section 8. The majority of this review is related to solution state NMR, however, Section 7 includes some contributions from solid-state ^{195}Pt NMR.

2. Methods

The signal-to-noise ratio, (S/N), of an NMR signal is given by[13]

$$\frac{S}{N} \propto NAT^{-1}B_0^{3/2}\gamma_{exc}\gamma_{obs}^{3/2}T_2^*(NS)^{1/2} \quad (1)$$

where N is the number of molecules in the observed sample volume, A is the abundance of the NMR active spins involved in the experiment, T is the temperature, B_0 is the static magnetic field, γ_{exc} and γ_{obs} represent the gyromagnetic ratios of the initially excited and the observed spins respectively, T_2^* is the effective transverse relaxation time and NS is the total number of accumulated scans. Due to the low γ of ^{195}Pt, direct observation of this nucleus generally results in low S/N.

The detection of less sensitive X-nuclei is challenging and many advances have been made to improve the NMR techniques for the detection of low γ nuclei.[14–16] Early methods for determining heteronuclear shift correlations were based on the direct observation of ^{195}Pt with ^{1}H being indirectly detected. During the last decade though, the approach to data collection has fundamentally changed to where the high γ-nucleus (for example, ^{1}H) is observed, and the heteronucleus is detected indirectly.[14–16] In particular, multi-dimensional ^{195}Pt NMR methods are gaining popularity for studying inorganic complexes. The most sensitive, and now routinely used, method for obtaining signals from less sensitive nuclei involves double-polarisation transfer (I→S→I), where I is the nuclei of interest and S is the spectator nuclei. Some standard two-dimensional NMR sequences involving heteronuclear multiple quantum correlation (HMQC) and heteronuclear single quantum correlation (HSQC) are shown in Fig. 1 and 2,

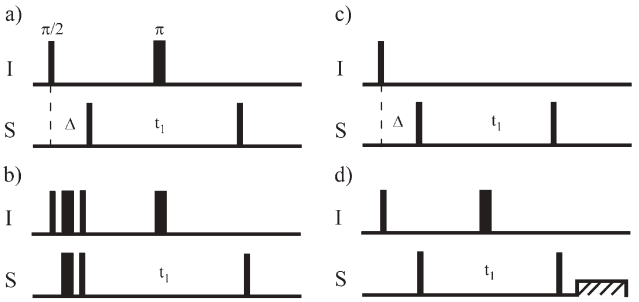

Fig. 1 HMQC pulse sequences (a) for small heteronuclear coupling constant, J(I,S), values, (b) for larger, resolved J(I,S) values and phase sensitive presentation, (c) zero or double quantum variant for the determination of the I-spin multiplicity, and (d) with refocussing and optional S-spin decoupling.[13,15] The delays Δ and t_1 are the J coupling evolution time and mixing period, respectively. The hashed pulse indicates decoupling.

Janice Aldrich-Wright

Janice Aldrich-Wright was born and raised in Sydney. She received her BAppSc (Hons) in 1980 from the University of Technology Sydney in physical chemistry and subsequently spent several years in industry. In 1993 she received a PhD from Macquarie University and her thesis was awarded the 1994 Cornforth Medal of the Royal Australian Chemical Society for annually the most outstanding PhD thesis submitted in a branch of chemistry in Australia. She took up an academic position at the University of Western Sydney prior to finishing her PhD, where she is now an Associate Professor in the School of Biomedical and Health Sciences. She has approximately 30 publications and is a co-inventor on 4 patents. Her research interests are firmly based in medicinal inorganic chemistry and coordination chemistry including the design and synthesis of mononuclear and multinuclear metal complexes for probing DNA, and chemotherapeutic metal complexes, particularly those including platinum.

William S. Price

William S. Price received his BSc (Hons) in 1986 and PhD in 1990 from the University of Sydney. His honours project involved using NMR to determine protein conformation. His PhD studies, with Prof. Philip W. Kuchel and Dr Bruce A. Cornell, were on NMR studies of red blood cells. He then undertook postdoctoral studies at the Institute of Atomic and Molecular Science in Taipei, Taiwan 1990–1993 (with Prof. Lian-Pin Hwang) and the National Institute of Advanced Industrial Science and Technology in Tsukuba, Japan 1993–1995 (with Prof. Kikuko Hayamizu). From 1995–1999 he was Chief Scientist at the Water Research Institute in Tsukuba, Japan. In 2000 he was a senior visiting scientist at the Royal Institute of Technology (KTH) in Stockholm. From 2001–2003 he was Professor of Chemistry at Tokyo Metropolitan University. In late 2003 he took up the chair of Nanotechnology at the University of Western Sydney. He has approximately 85 publications. His research interests include pulsed gradient spin-echo NMR diffusion measurements, NMR microscopy, spin relaxation, water suppression and solid state ^{2}H studies.

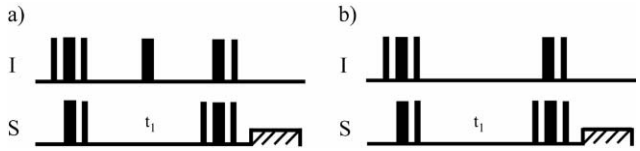

Fig. 2 HSQC pulse sequences with optional decoupling of the S-spin (a) for a standard sequence and (b) modified for the I-spin multiplicity determination.[13,15] The delay t_1 is the mixing period.

respectively.[16] Both HMQC and HSQC methods (see ref. 13,15) are used to correlate coupled heteronuclear spins across a single bond and hence identify directly connected nuclei, for example ^{1}H–^{195}Pt.

All the sequences presented in Fig. 1 and 2 provide a theoretical signal enhancement of $(\gamma_I/\gamma_S)^{5/2}$.[16] Commonly it is desirable to measure heteronuclear coupling constants (*i.e.*, $^nJ(X,^1H)$ interactions where n = 1–5). Usually though, n = 1–3 and X = ^{195}Pt, and the data is collected using the proton signals (for example, see Fig. 3).[17] Also, an HMQC experiment, where ^{31}P is the high γ-nuclei used for polarisation transfer, has been employed to study platinum–phosphine clusters.[18] $^2J(^{31}P,^{195}Pt)$ values were used to determine the delay Δ (= ½ ^2J (^{31}P,^{195}Pt); see Fig. 1c), to generate multiple quantum coherences.

3. Chemical shifts

3.1 Theoretical studies

Although there are well-established empirical rules to describe and interpret δ^{195}Pt,[19] methods rooted in density functional theory (DFT) are particularly appealing due to their remarkable accuracy coupled with their efficiency in handling electron correlation.[20,21] General chemical shift theory[19,22] describes the chemical shift tensor (σ_t) as a combination of paramagnetic (σ_p), diamagnetic (σ_d) and extraneous (σ_x) components and hence

$$\sigma_t = \sigma_p + \sigma_d + \sigma_x \quad (2)$$

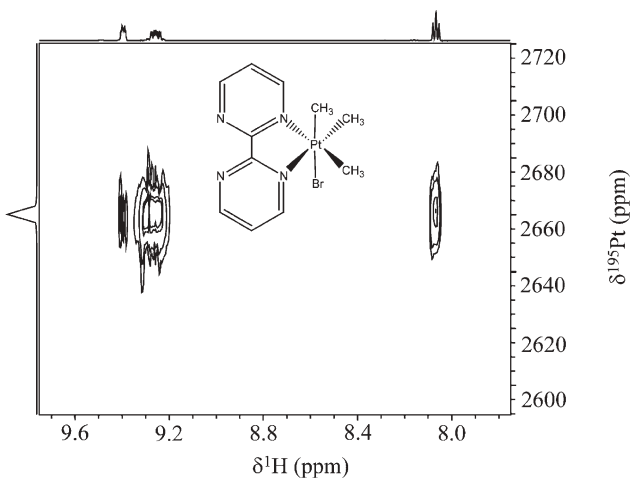

Fig. 3 Expansion of the ^{1}H,^{195}Pt-HMQC spectrum of the Pt–bipyrimidine complex (inset) displaying correlation *via* $^3J(^1H,^{195}Pt)$, $^4J(^1H,^{195}Pt)$ and $^5J(^1H,^{195}Pt)$ from all the three different protons in the pyrimidine ring.[17]

with σ_p generally being the dominant term due to low-lying excited electronic states.[22–25] Studies of σ_p for ^{195}Pt date from the 1950s when Ramsey's equation for paramagnetic shielding[22] was applied to square planar D_{4h} $[PtX_4]^{2-}$ systems.[26,27] Using visible absorption and ^{195}Pt NMR data it was argued that the covalency of the platinum ligand bond has a greater influence on δ^{195}Pt than orbital energy gaps.[2,28] The relative covalency of various ligands in a series of $[PtX_3L]^-$ anions was determined.[29] Later, Appleton *et al.*[30] rationalised δ^{195}Pt in several *pseudo*-square-planar Pt(II) systems. A correlation between the electronic spectra and (a) changes in δ^{195}Pt as a function of R and R′ and (b) the solvent dependence of δ^{195}Pt for Pt(0) complexes of the type $[Pt(R–C\equiv C–R')(PPh_3)_2]$ was determined in 1981 by Koie *et al.*[31] By extending the general chemical shift expression to include spin–orbit relativistic effects Gilbert and Ziegler[27] have obtained the following expression for σ_t:

$$\sigma_t = \sigma_p + \sigma_d + \sigma_x + \sigma_{so} \quad (3)$$

where σ_{SO} describes the contribution from spin–orbit relativistic effects. In this study, DFT was used to calculate δ^{195}Pt for a series of Pt(II) complexes which were then confirmed by experiment. Good agreement with experimental values was observed with two different methods to describe σ_{SO} (a) a zeroth order regular approximation (ZORA) method[32] and (b) a Pauli Hamiltonian method.[33] Two trends in δ^{195}Pt could be seen (1) an experimental trend that iodides resonate at a lower frequency (low ppm or high field) than chlorides and (2) a computational trend that *cis* isomers resonate at lower frequencies than *trans* isomers.

The contribution from σ_{SO} to δ^{195}Pt is negative and increases considerably in absolute terms from chlorine to iodine. This trend is displayed graphically in Fig. 4 for the *cis*- and *trans*-$[PtX_2(PMe_3)_2]$ series. The contribution of σ_{SO} is clearly significant in explaining these trends and in only a few cases can δ^{195}Pt be accurately calculated without it.

Fowe *et al.*[34] used the ZORA spin–orbit Hamiltonian in conjunction with a modified DFT method to calculate the δ^{195}Pt of $[PtCl_xBr_{6-x}]^{2-}$ complexes (Table 1). The authors found that δ^{195}Pt was dominated by σ_p and σ_{SO}, whereas σ_d

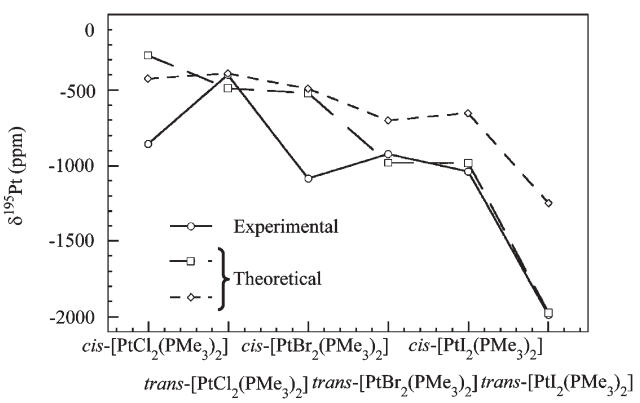

Fig. 4 Plot of experimental (–○–) and calculated (using the Pauli Spin–Orbit (–□–) and Pauli Scalar (–◇–) models) δ^{195}Pt for a series of $[PtX_2(PMe_3)_2]$ complexes.[27]

Table 1 Different contributions (paramagnetic, diamagnetic, spin–orbit/Fermi contact (SO/FC)) to the δ^{195}Pt (ZORA formalism) values[34]

Compound	δ^{p}/ppm	δ^{d}/ppm	$\delta^{SO/FC}$/ppm	δ_{calc}/ppm	δ_{expt}/ppm	Δ/ppm
$[PtCl_6]^{2-}$	0	0	0	0	0	0
$[PtCl_5Br]^{2-}$	−166.7	0.6	−110.7	−276.8	−282	5.2
Trans-$[PtCl_4Br_2]^{2-}$	−326.4	1.2	−258	−583.3	−583.6	0.3
Cis-$[PtCl_4Br_2]^{2-}$	−344	1.2	−222.8	−565.6	−582.4	16.8
Fac-$[PtCl_3Br_3]^{2-}$	−531.0	1.8	−336.6	−865.8	−889.2	23.4
Mer-$[PtCl_3Br_3]^{2-}$	−516.5	1.8	−372.6	−887.6	−891.4	3.8
Trans-$[PtCl_2Br_4]^{2-}$	−699.5	2.4	−526.1	−1223.3	−1210	−13.3
Cis-$[PtCl_2Br_4]^{2-}$	−714.3	2.4	−489.3	−1201.2	−1210	8.8
$[PtClBr_5]^{2-}$	−908.3	3.0	−645.6	−1551.7	−1540	−11.5
$[PtBr_6]^{2-}$	−1113.5	3.6	−805.4	−1915.2	−1870	−45.2

was negligible. They also found a strong dependence of δ^{195}Pt on the bond lengths (see Fig. 5) and solvation effects.

Solvation effects have also been shown to be important determinants of δ^{195}Pt. Theoretical studies of σ_t for platinum–thallium (Pt–Tl) based transition metal complexes (see Fig. 6 and 7) have shown that it is necessary to include solvation effects when calculating δ^{195}Pt since solvent molecules bind to the metal centre and affect the coordination sphere.[35–37] DFT based methods have led to reliable predictions of δ^{195}Pt values and show that the effects of the solvent (H_2O) on the NMR observables turn out to be remarkably large.[36]

3.2 Experimental studies

There are a number of difficulties in referencing metals and in particular platinum transition metal complexes. A number of key features of platinum NMR referencing have been noted by Pregosin:[38] (a) the relatively large temperature dependence (broad-band ^{1}H-decoupling can cause a temperature change) of the chemical shift—several tenths of a ppm per degree is not unusual, (b) their interactions with solvent and/or substance added as internal reference, (c) uncertainties due to isotopomers and (d) relatively small mathematical errors associated with the choice of divisor. δ^{195}Pt are normally expressed relative to a standard sample, $[PtCl_6]^{2-}$ or $[PtCl_4]^{2-}$, in D_2O (usually $>$ 10 mM for direct observation), however, referencing can also be made to $[Pt(CN)_6]^{2-}$. The approximate range of δ^{195}Pt for Pt(0), Pt(II) and Pt(IV) complexes have been established and are depicted in Fig. 8. The ranges are inclusive

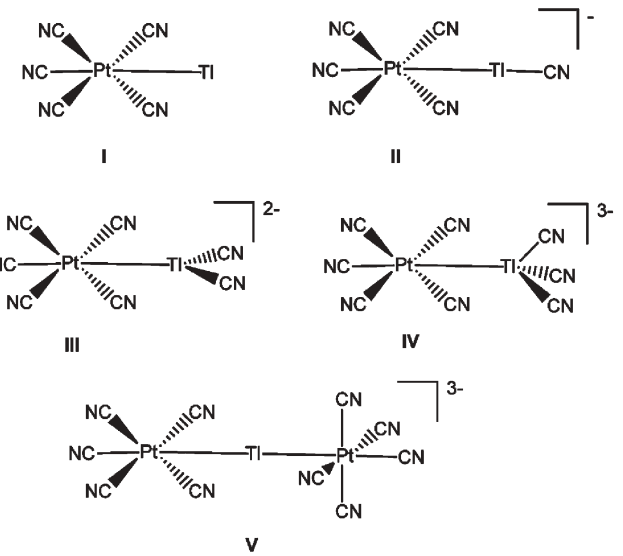

Fig. 6 Proposed structures of a series of Pt–Tl complexes by Autschbach *et al.*[36]

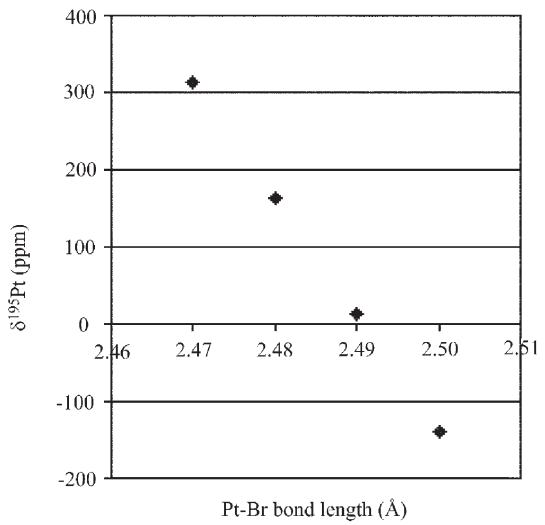

Fig. 5 Calculated influences of δ^{195}Pt with Pt–Br bond length in $[PtBr_6]^{2-}$.[34]

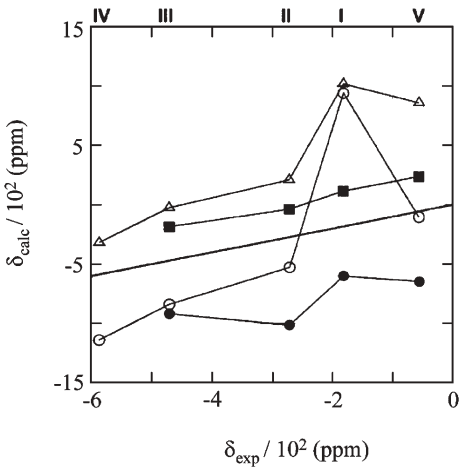

Fig. 7 Comparison of calculated and experimental δ^{195}Pt (using $[Pt(CN)_6]^{2-}$ as chemical shift reference) using ○ = unsolvated; ● = explicit first solvation shell (A); △ = conductor-like screening model (COSMO); ■ = (A) + COSMO for second solvation shell models.[37]

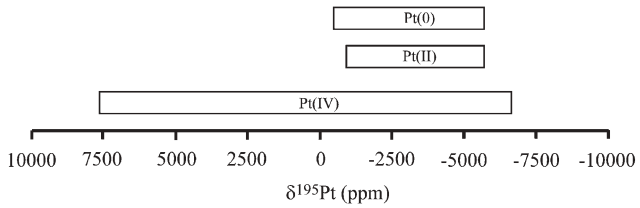

Fig. 8 Approximate range of δ^{195}Pt for different oxidation states. The chemical shifts are relative to $[PtCl_6]^{2-}$ in D_2O.

of the steric effects on replacing different ligands and the structural change on varying the temperature. Intermediate reactive species of Pt(III) compounds have also been characterised by trends in δ^{195}Pt. The calculated shift of Pt(0) is −10,427 ppm,[39] and removal of electrons to give Pt(II) leads to deshielding and high-frequency shifts. Pt(IV) resonances tend to resonate at the high-frequency end of the NMR spectrum, but there is considerable overlap.

Trends for a range of ligand substituents including halogens, amines, phosphines, heterocycles (including pyridine and macrocycles) and arsenic and sulfur ligands have now been established. Some of the prominent trends as noted by Pregosin[3] are summarised in Fig. 9 and 10.

More specialised ligand substituents and their influence on the chemical shift of platinum can be seen in the following examples and are shown in Fig. 11:

A. The order of increased shielding of ^{195}Pt for related amine complexes is $OSO_3^{2-} < OH^- < H_2O < Cl^- < NO_2^- < Br^- < NH_3 < SCN < I <$ tu (solid thiourea) $< Me_2SO$–S. For example, *cis*-$[Pt(^{15}NH_3)_2(H_2O)_2]$, *cis*-$[Pt(^{15}NH_3)_2(^{15}NO)_2]$ and *cis*-$[Pt(^{15}NH_3)_2(SCN)_2]^{2-}$ appear at −1593, −2214 and −3016 ppm, respectively.[30]

B. Increasing the number of $SnCl_3^-$ ligands per platinum centre results in increased shielding of ^{195}Pt. For example $[PtCl_3(SnCl_3)]^{2-}$, *cis*-$[PtCl_2(SnCl_3)_2]^{2-}$, $[PtCl(SnCl_3)_3]^{2-}$ and $[Pt(SnCl_3)_4]^{2-}$ appear at −2748, −4202 , −4829 and −5615 ppm, respectively.[40]

C. Increased phosphine ligand size results in deshielding of ^{195}Pt. It has been noticed that the ^{195}Pt resonance shifts

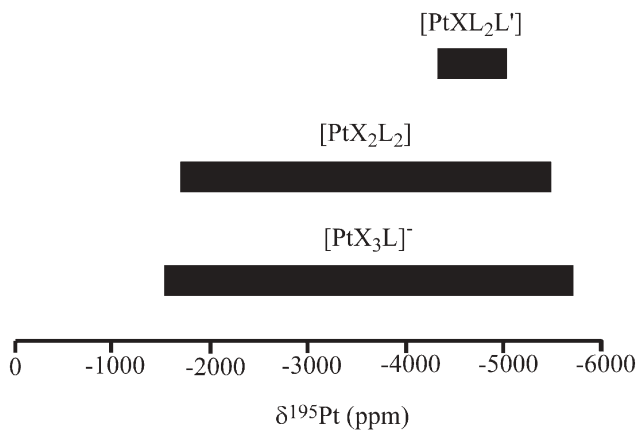

Fig. 9 Approximate range of δ^{195}Pt for a series of Pt complexes where X = Cl, Br, I and L = N, P, As, Sb, S, Se and Te-ligand substituents.

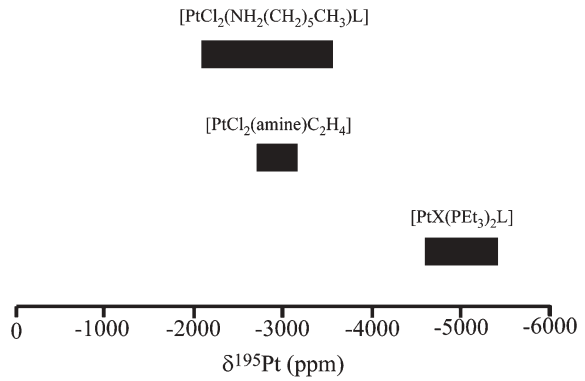

Fig. 10 Approximate range of δ^{195}Pt for a series of Pt complexes where X = Cl, Br, I and L = Si, Ge, Sn, N, P and As-ligand substituents.

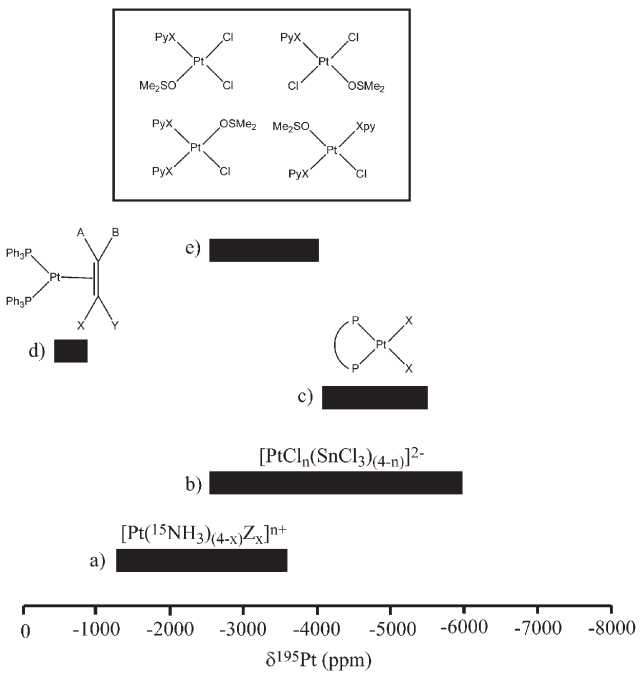

Fig. 11 Approximate range of δ^{195}Pt for a series of Pt complexes with various ligand substituents and their influence on δ (a) Pt–amine complexes[30] (b) Pt–Sn complexes[40] (c) Pt–phosphine complexes[3] (d) Pt–alkene complexes[42] (e) Pt–pyridine complexes.[43]

downfield when the size of the phosphines is increased which suggests a deshielding effect associated with a lengthening of Pt–P bonds.[3,41]

D. In a series of $[Pt(PPh_3)_2(alkene)]$ compounds containing asymmetric olefins the CN substituent has a stronger influence on δ^{195}Pt than substituents like $COOCH_3$, Ph or OEt. This trend in δ^{195}Pt has been seen in the series $[Pt(PPh_3)_2C_2H_{4-n}(CN)_n]$ and $[Pt(PPh_3)_2C_2H_{4-n}(COOCH_3)_n]$.[42]

E. The *ortho* substituent on pyridine ligands results in shielding of ^{195}Pt in the order $O^- >$ NHR $> CH_3O \sim HOCH_2 \sim CH_3 \sim C_2H_5 \sim$ n-$C_3H_7 >$ HC(O) $> (C_6H_5)C(O) \sim$ 3-thienyl $> C_6H_5$. Marzilli *et al.*[43] demonstrated that there is a dependence of shift on heterocyclic ligand basicity and also on the *ortho* substituent of pyridine in complexes of *cis*-$[Pt(Xpy)(Me_2SO)Cl_2]$, *trans*-$[Pt(Xpy)(Me_2SO)Cl_2]$,

cis-$[Pt(Xpy)_2(Me_2SO)Cl]^+$ and *cis*-$[Pt(Xpy)(Me_2SO)_2Cl]^+$ where X is the above mentioned ligands. The data collected showed that there is an upfield shift as the basicity of the pyridine increases for *cis*-$[Pt(Xpy)(Me_2SO)Cl_2]$, *cis*-$[Pt(Xpy)_2(Me_2SO)Cl]^+$ and *cis*-$[Pt(Xpy)(Me_2SO)_2Cl]^+$ but the opposite trend is observed for *trans*-$[Pt(Xpy)(Me_2SO)Cl_2]$.

It is convenient to sub-divide the further discussion of δ^{195}Pt according to the oxidation state of Pt.

3.2.1 Pt(0) complexes. Asaro *et al.*[42] have shown that δ^{195}Pt is affected by olefin substitution in several phosphine complexes (See Fig. 12). δ^{195}Pt and coupling constants of the metal to bound phosphorus atoms are summarised in Table 2. A difference in ^{31}P–^{195}Pt coupling constants was observed in the case of asymmetric olefins, however, the $^1J(^{13}C,^{195}Pt)$ values indicate that the metal interacts strongly with C(1) rather than C(2) (see Fig. 12). The studies thus confirmed the importance of back-donation of Pt(0) to olefin compounds.

Dotta *et al.*[44] have reported several mono-dentate phosphine (MOP) complexes, where two MOP ligands bind to Pt and the third ligand is diphenylacetylene. ^{195}Pt NMR spectra (at low temperature) revealed the triplet multiplicity expected for a bis-phosphine complex with $^1J(^{31}P,^{195}Pt)$ = 3590 Hz and δ^{195}Pt = −4968 ppm in dichloromethane.

3.2.2 Pt(II) complexes. The resonances of Pt(II) complexes are found in the same range as for Pt(0) complexes. Barnham *et al.*[45] devised a useful empiricism which involves δ^{195}Pt and/or coupling constants in square planar and octahedral complexes (see Fig. 13 for the general structure of each complex). They noted that there is often a dependence of either δ^{13}C, ^{14}N or ^{31}P on the $^1J(^{195}Pt$, spin = 1/2 nucleus) on the *trans* influence of the ligand, L. For strong L-donors the chemical shift moves to lower frequencies and $^1J(^{195}Pt$, spin = 1/2 nucleus) can be markedly reduced. This is the case for the square-planar Pt(II) complexes, with the ligand being NH_3 (or

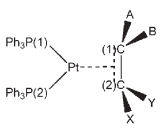

	A	B	X	Y
1	H	H	H	H
2			η^2-C_{60}	
3	H	H	H	CN
4	H	*p*-NO_2-Ph	$COOCH_3$	CN
5	H	Ph	$COOCH_3$	CN
6	H	Ph	CN	CN
7	H	OEt	CN	CN

Fig. 12 A series of Pt–phosphine complexes with different olefin ligands.[42]

Table 2 Chemical shifts and coupling constants values for complexes **1–7** from Fig. 12[42]

	δ^{195}Pt/ppm	$^1J(^{31}P_1,^{195}Pt)$/Hz	$^1J(^{31}P_2,^{195}Pt)$/Hz
1	−542	3721	3721
2	—	3933	3933
3	−534	3965	3481
4	−535	4302	3443
5	−541	4438	3360
6	−445	4344	3268
7	−446	4486	2988

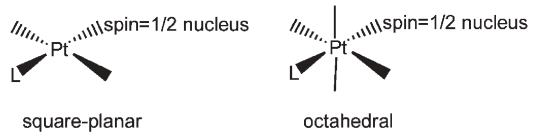

Fig. 13 General conformations of square-planar (left) and octahedral (right) Pt-complexes.

a substituted amine). It has been suggested that O, N and S-donors in the *trans* position can be distinguished by δ^{15}N and/or δ^{195}Pt.[16,45]

In ^{195}Pt NMR, the diiodo complexes are observed at much higher fields than the dichloro analogues (for example, see Fig. 4).[46–48] Data obtained from a recent study by Rochon and Buculei on *cis*- and *trans*-$[Pt(amine)_2I_2]$ involving primary and secondary amines are summarised in Tables 3, 4 and 5.[48]

δ^{195}Pt for *cis*-diiodo complexes with primary amines were observed between −3342 and −3357 ppm in acetone, while the *trans* complexes were found between −3336 and −3372 ppm (see Table 3). For secondary amines, δ^{195}Pt was observed at higher frequencies. As shown in Table 5, the $^3J(^1H,^{195}Pt)$ coupling constants in the $[PtI_2(amine)_2]$ complexes are larger for the *cis* isomers (45 Hz) than for the *trans* isomers (36 Hz). The $^2J(^1H,^{195}Pt)$ coupling constants of the amine protons are also larger in the *cis* isomers (67 *versus* 59 Hz). The $^3J(^{13}C,^{195}Pt)$ coupling constants are known to be geometry dependent and their average values were found to be 38 and 27 Hz for the *cis* and *trans* compounds, respectively. Further, $^2J(^{13}C,^{195}Pt)$ coupling constants were found be small, 17 (*cis*) and 11 (*trans*) Hz, but still observable in the ^{13}C NMR spectra. The dependence of the pK_a values of the protonated amines or the proton affinity (PA) in the gas phase with the δ^{195}Pt values are shown in Fig. 14 and 15, respectively.

The reactions of platinum(II) aqua complexes involving diamine ligands were investigated with various oxygen-donor anions like hydroxide, perchlorate, nitrate, sulfate, phosphate and acetate.[49,50] ^{195}Pt NMR studies were used to study the equilibria between the aqua complexes and substituted anions.

In a series of papers Farrell and coworkers[51–58] have used ^{195}Pt NMR to characterise various platinum amine complexes. These complexes showed anti-tumour activity by binding to DNA and have shown promise in chemotherapy. In one of

Table 3 Chemical shifts δ^{195}Pt, proton affinity (PA), pK_a values and $\Delta\delta(\delta_{cis} - \delta_{trans})$ of the $[PtI_2X_2]$ complexes in acetone-d_6[48]

X	PA	pK_a	*Cis*/ppm	*Trans*/ppm	$\Delta\delta$/ppm
$MeNH_2$	914	10.62	−3342	−3360	18
			−3324[a]	−3348[a]	24[a]
$EtNH_2$	930	10.63	−3354	−3368	14
			−3328[a]	−3353[a]	25[a]
n-$PrNH_2$	933	10.69	−3350	−3363	13
n-$BuNH_2$	924	10.61	−3349	−3363	13
iso-$PrNH_2$	—	10.63	−3352	−3345	−7
iso-$BuNH_2$	—	10.72	−3357	−3372	15
sec-$BuNH_2$	—	10.56	−3346	−3336	−10
			−3309	−3322	13[a]
t-$BuNH_2$	—	10.68	—	−3369	—
Me_2NH	—	10.73	−3247	−3057	−190
Et_2NH	—	11.04	−3302	−3128	−174

[a] In DMF-d_7.

Table 4 δ^{195}Pt and $\Delta\delta$ ($\delta_{cis} - \delta_{trans}$) of the $[PtI_2X_2]$ complexes in DMF-d_7[48]

Complex	*Cis*/ppm	*Trans*/ppm	$\Delta\delta$/ppm
$[Pt(NH_3)_2I_2]$	−3264[a]	—	—
	−3198	—	—
$[Pt(MeNH_2)_2I_2]$	−3327	—	—
$[Pt(EtNH_2)_2I_2]$	−3330	—	—
$[Pt(Me_2NH)_2I_2]$	−3327	—	—
[Pt(1-adam)$_2$I$_2$]	−3364	−3331	−33
[Pt(2-adam)$_2$I$_2$]	−3333	—	—
[Pt(cpa)$_2$I$_2$]	−3302	—	—
[Pt(cba)$_2$I$_2$]	−3346	—	—
[Pt(cba)(2-adam)I$_2$]	−3387	−3358	−29
$[Pt(Me_2NH)(1\text{-adam})I_2]$	−3389	−3336	−53
[Pt(py)$_2$I$_2$]	−3199[a]	−3133	−66
[Pt(Ypy)$_2$I$_2$] (δ_{ave})	−3235[a,b]	−3161	−74
$[Pt(NH_3)_2Cl_2]$	−2104	−2101	−3
	−2100	−2101	1
	−2097	—	—
$[Pt(MeNH_2)_2Cl_2]$	−2222	—	—
$[Pt(Me_2NH)_2Cl_2]$	−2188	−2181	−7
[Pt(*iso*-PrNH$_2$)$_2$Cl$_2$]	−2224	—	—
$[Pt(C_6H_{11}NH_2)_2Cl_2]$	−2215[c]	−2130[a]	−85
[Pt(cpa)$_2$Cl$_2$]	−2235	—	—
[Pt(1-adam)$_2$Cl$_2$]	−2184	−2141	−43
[Pt(2-adam)$_2$Cl$_2$]	−2230	−2193	−37
[Pt(1-Meadam)$_2$Cl$_2$]	−2242	—	—
[Pt(py)$_2$Cl$_2$]	−2014[a]	−1960	−54
[Pt(Ypy)$_2$Cl$_2$] (δ_{ave})	−2009[a]	−1957	−52

[a] $CDCl_3$. [b] CD_2Cl_2. [c] DMSO, cpa = cyclopropyl amine, cba = cyclobutyl amine, adam = adamantane, δ_{ave} = average chemical shift.

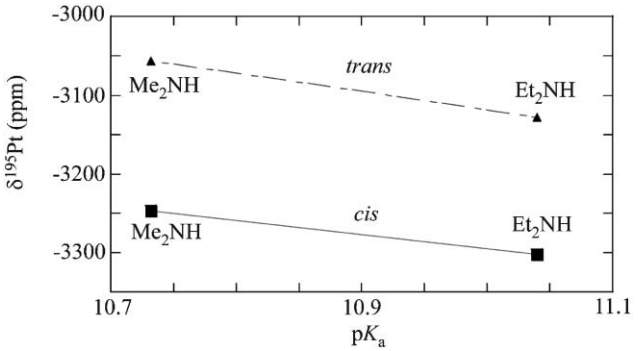

Fig. 14 δ^{195}Pt *vs.* pK_a of the protonated amines for the *cis* and *trans* complexes of $[PtI_2X_2]$ (X = secondary amines).[48]

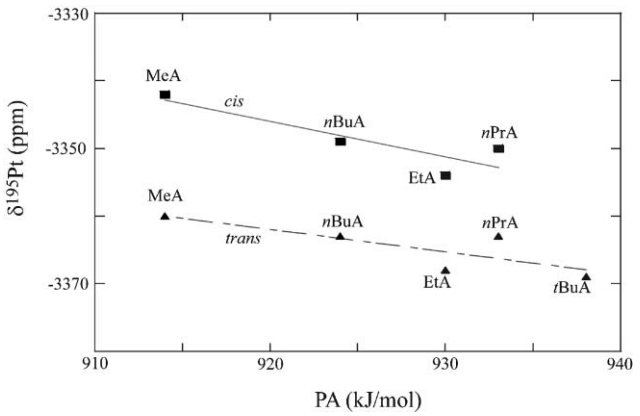

Fig. 15 δ^{195}Pt *vs.* proton affinity (PA) of the amines for the *cis* and *trans* complexes of $[PtI_2X_2]$.[48]

their studies[56] the isomerisation of $[(trans\text{-}PtCl_2(Me_2SO))_2\text{-}NH_2(CH_2)_4NH_2]$ to the dinuclear *cis* derivative was followed by ^{195}Pt NMR (see Fig. 16).

δ^{195}Pt of several organoplatinum compounds in solution have been determined.[59] The δ^{195}Pt of various phosphine Pt(II) and Pt(0) compounds lie in separate ranges, and allow the metal–diene system to be characterised either as metallacyclopentene or as an η^2-bonded diene.

The mononuclear complexes of $[PtCl_2X_2]$ (X = substituted phosphines) were investigated by Münzenberg *et al.*[60] It was shown that the *cis*-influence on the platinum aminophosphine bond was characterised by the $^1J(^{31}P,^{195}Pt)$ coupling constant, whereas X-ray analyses failed to detect the small *cis*-influence because the Pt–P bond lengths vary only by about 1 pm. δ^{195}Pt for the Pt(II)-phosphine complexes were around −2800 ppm and identified by a doublet of doublets because of the metal coupling to both phosphorus atoms. Although $^1J(^{31}P,^{195}Pt)$ values can be more than 6000 Hz,[3] in this study they were

Table 5 Coupling constants with ^{195}Pt of the $[PtI_2X_2]$ complexes[48]

X	Isomer	$^2J(^1H,^{195}Pt)$/Hz	$^3J(^1H,^{195}Pt)$/Hz	$^2J(^{13}C,^{195}Pt)$/Hz	$^3J(^{13}C,^{195}Pt)$/Hz
$MeNH_2$	*Cis*	69	49	21	—
	Trans	61	35	15	—
$EtNH_2$	*Cis*	68	—	18	48
	Trans	58	—	12	36
n-$PrNH_2$	*Cis*	68	—	17	45
	Trans	59	—	10	36
n-$BuNH_2$	*Cis*	65	43	18	43
	Trans	58	—	12	34
iso-$PrNH_2$	*Cis*	66	—	13	30
	Trans	60	—	11	22
iso-$BuNH_2$	*Cis*	66	—	18	—
	Trans	59	—	14	—
sec-$BuNH_2$	*Cis*	67	—	—	32, 24
	Trans	—	—	10	28, 21
t-$BuNH_2$	*Trans*	58	—	9	17
Me_2NH	*Cis*	70	43	14	—
	Trans	62	37	10	—
Et_2NH	*Cis*	68	—	13	34
	Trans	60	—	9	22

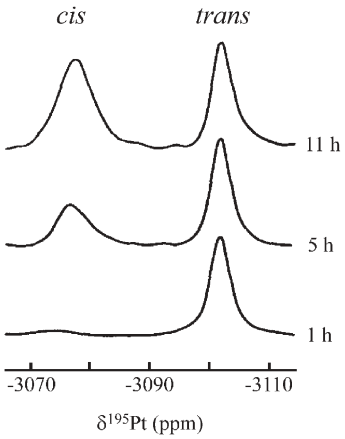

Fig. 16 Isomerisation of the *cis* and *trans* complexes of $[Pt\{Cl_2(Me_2SO)_2\}\mu\text{-}NH_2(CH_2)_4NH_2]$ in DMSO-d_6 followed by ^{195}Pt NMR.[56]

found in the range of 3500–4100 Hz. The decrease in the coupling constant indicated weak Pt–P σ-bonds and thus the *cis*-influence was characterised. Indeed the magnitude of the *cis*-influence is only a fifth of a normal *trans*-influence found for *cis*/*trans* isomers of Pt(II)–phosphine complexes.[61]

A study on L-serine–Pt(II) complexes has been reported by Watabe *et al.*[62] Their intention was to find the difference in reactivities of *cis* and *trans*-[Pt(L-Ser–N,O)$_2$] (*i.e.*, a and e, respectively in Scheme 1) complexes with HCl. Both ^{195}Pt NMR (see Table 6 and Fig. 17 and 18) and high performance liquid chromatography (HPLC) confirmed that the coordinated carboxyl oxygen atoms of the *trans* isomer detached faster than that of the *cis* isomer. The difference in $\delta^{195}Pt$ between *cis*-[PtCl$_2$(L-Hser–N)$_2$] and *trans*-[PtCl$_2$(L-HSer–N)$_2$] (see Table 6 and structures g and c in Scheme 1) is only 40 ppm, and is larger than that between *cis*-[PtCl$_2$(NH$_3$)$_2$] ($\delta^{195}Pt$ = −2123 ppm) and *trans*-[PtCl$_2$(NH$_3$)$_2$] ($\delta^{195}Pt$ = −2101 ppm).[61,63]

Table 6 $\delta^{195}Pt$ [a] for Pt(II) complexes containing L-serine (see Scheme 1 and Fig. 17 and 18)[62]

Pt(II) complex	δ_{Pt}^{obsd}/ppm	Letter in Scheme 1 in Fig. 17 and 18
Trans-[Pt(L-Ser–N,O)$_2$]	−1632	e
K[PtCl$_2$(L-Ser–N,O)]	−1633	x
Cis-[Pt(L-Ser–N,O)$_2$]	−1832	a
K[PtCl$_3$(L-HSer–N)]	−1964[b]	d
Trans-[PtCl(L-Ser–N,O)(L-HSer–N)]	−1975[b]	f
Cis-[PtCl(L-Ser–N,O)(L-HSer–N)]	−1974[b]	b
Trans-[PtCl$_2$(L-HSer–N)$_2$]	−2220[b]	g
Cis-[PtCl$_2$(L-HSer–N)$_2$]	−2261[b]	c

[a] Shifts are relative to Na$_2$[PtCl$_6$], [b] Obtained from the reaction mixture containing HCl in Fig. 17 and 18 in which the corresponding complex predominantly existed.

In a study of the reactivity of glutathione with Pt(II) antitumor compounds, the change of $\delta^{195}Pt$ upon addition of glutathione was used to monitor transplatin analogues.[64] This study showed that $\delta^{195}Pt$ shifts to lower frequency with increasing glutathione concentration. When all the Cl^- ligands have been replaced, however, a bridged (*via* S) species is formed which exhibits a higher frequency shift.

The solvolyses of the complexes *cis*-[Pt(L$_2$)X$_2$], where L$_2$ is two NH$_3$ molecules or ethylenediamine and X = Cl^-, Br^-, or I^-, has been studied in DMSO by ^{195}Pt NMR.[65] This study is

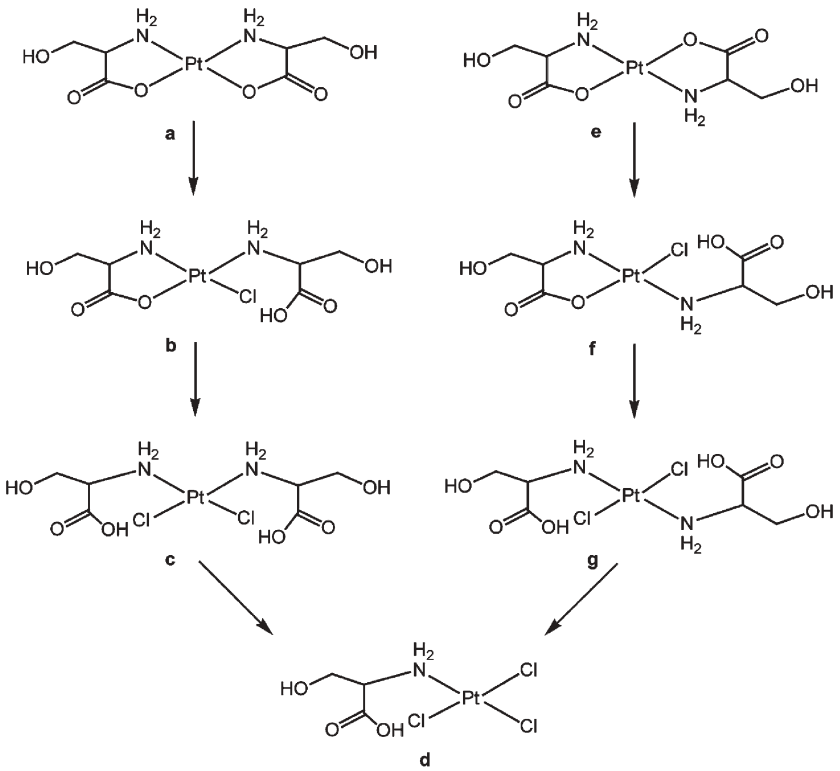

Scheme 1 Reaction scheme showing the detachment of the oxygen atom from the chelated carboxyl oxygen of *cis* and *trans*-[Pt(L-Ser–N,O)$_2$].[62]

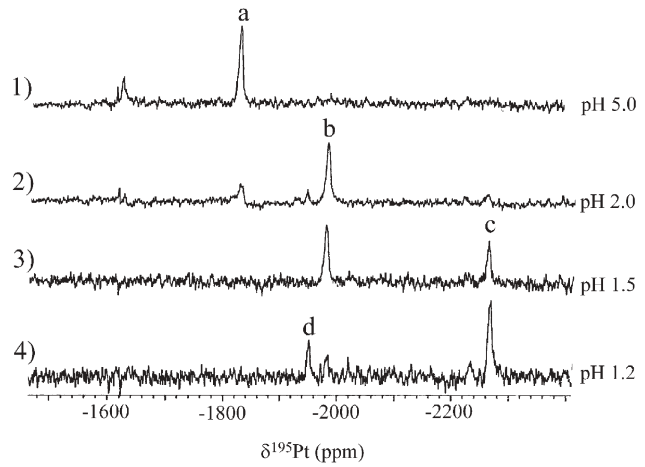

Fig. 17 ^{195}Pt NMR spectra for the reaction of *cis*-[Pt(L-Ser–N,O)$_2$] with HCl at (1) 0 min; (2) 5 min; (3) 10 min; and (4) 15 min at 80 °C.[62]

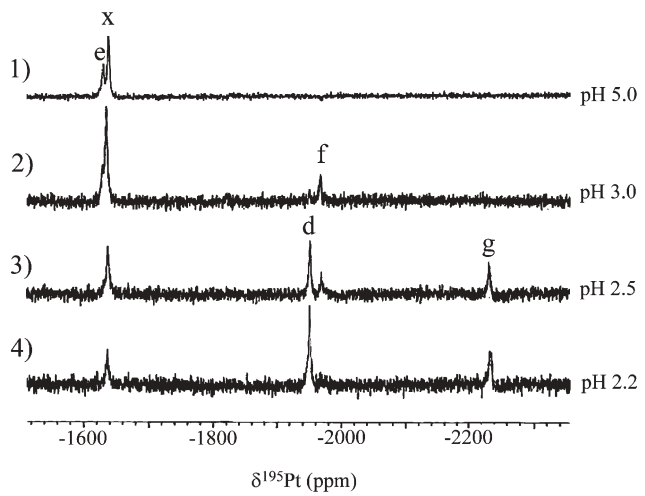

Fig. 18 ^{195}Pt NMR spectra for the reaction of *trans*-[Pt(L-Ser–N,O)$_2$] containing [PtCl$_2$(L-Ser–N,O)$_2^-$] with HCl at (1) 0 min; (2) 5 min; (3) 10 min; and (4) 15 min at 80 °C.[62]

of biological interest (anticancer screening) since Pt(II) DMSO complexes of the type *cis*-[Pt(amine)$_2$(DMSO)$_2$] are more water soluble and less toxic than the analogous halide complexes.

The head-to-head to head-to-tail isomerisation of α-pyridonate-bridged ethylenediamineplatinum(II) dimer has been studied using ^{195}Pt NMR.[66,67] The studies revealed the occurrence of a reversible, intramolecular, dissociatively activated stereochemical rearrangement.

The chemistry of platinum(II) with CO and $SnCl_3$ ligands has been studied.[68] The presence of ^{119}Sn satellites in the ^{195}Pt spectrum was used to determine the structure of the complexes and the coupling was used to confirm the existence of a Pt–$SnCl_3$ bond.

3.2.3 Pt(III) complexes. Binuclear species comprise the vast majority of the structurally characterised platinum(III) complexes and therefore provide the best opportunity for probing the structural properties and chemical reactivity of this oxidation state.[69] The influence of steric interactions on structure and reactivity in [Pt$_2$(en)(C$_5$H$_4$NO)$_2$](NO$_3$)$_2$ complexes have been noted by Lippard and coworkers.[69] δ^{195}Pt were used to confirm the binuclear metal–metal bond with a nitrite/nitrate-capping framework. The ^{195}Pt NMR spectra of platinum(III) complexes with sulfato- and phosphato-bridged ligands have been reported.[70] The effects of axial ligand substituents on the spectra were discussed and it was seen that there was a similarity in the J(^{195}Pt–^{195}Pt) couplings of the closely related complexes under study.

3.2.4 Pt(IV) complexes. The chemical shifts for Pt(IV) complexes often appear at higher frequency compared to Pt(II) and Pt(0) complexes. For example, [PtCl$_6$]$^{2-}$ = 0 whereas [PtCl$_4$]$^{2-}$ = −1620; [PtBr$_6$]$^{2-}$ = −1860 and [PtBr$_4$]$^{2-}$ = −2690; [Pt(CN)$_6$]$^{2-}$ = −3866 and [Pt(CN)$_4$]$^{2-}$ = −4746 ppm. Fig. 19 shows the regular, low-frequency shifts of the ^{195}Pt resonances on stepwise addition of the Cl-ligands of the [PtCl$_6$]$^{2-}$ and [PtCl$_4$]$^{2-}$ by Br$^-$.[71] Further, it is known that the Pt(IV) halides alone span some 12500 ppm. For example, δ^{195}Pt [PtF$_6$]$^{2-}$ = 7326, δ^{195}Pt [PtCl$_6$]$^{2-}$ = 0, δ^{195}Pt [PtBr$_6$]$^{2-}$ = −1860 and δ^{195}Pt [PtI$_6$]$^{2-}$ = −5120 ppm.

There is considerable interest in the coordination of nitrogen ligands to a Pt(IV) centre.[72] New Pt(IV) and Pt(II)–oxadiazole complexes have been synthesised *via* the activation of an RC–N bond and characterised by mass and NMR spectroscopy.[73] ^{195}Pt NMR was used to determine the oxidation state of the metal, where Pt(IV) chemical shifts were in the range of −170 to 20 and Pt(II) was around −2200 ppm.

Watabe *et al.*[74] have isolated [Pt(diGly)Cl$_3$]$^-$ (see Fig. 20) and [Pt(Gly-L-α-Ala)Cl$_3$]$^-$ dipeptide (dipep) complexes which showed a higher anti-fungal activity than cisplatin. The ^{195}Pt NMR peaks of [Pt(dipep)Cl$_3$]$^-$ and [Pt(Hdipep)Cl$_3$]$^-$ appeared at about 270 and −130 ppm, respectively (see Table 7), and were predicted for a given set of ligands (Fig. 21).

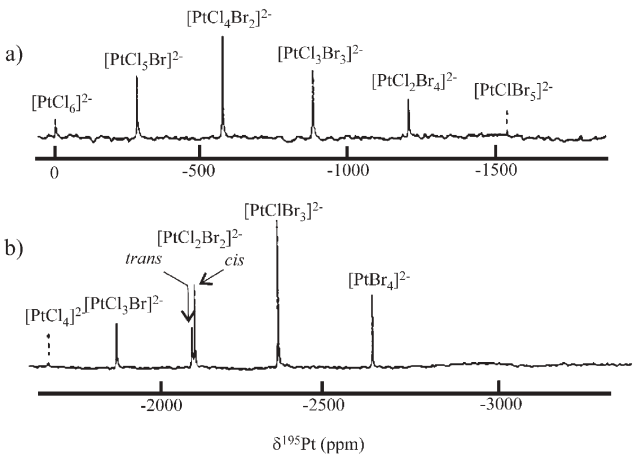

Fig. 19 ^{195}Pt NMR spectra of Pt(IV) and Pt(II) chloro–bromo complexes. (a) Na$_2$[PtCl$_6$] (1 M) in D$_2$O plus 2 equiv. of NaBr. At higher resolution the resonances of [PtCl$_4$Br$_2$]$^{2-}$, [PtCl$_3$Br$_3$]$^{2-}$ and [PtCl$_2$Br$_4$]$^{2-}$ are resolved into 4:1, 2:3 and 4:1 doublets, respectively; (b) K$_2$[PtCl$_4$] (0.4 M) in D$_2$O plus 4 equiv. of NaBr.[71]

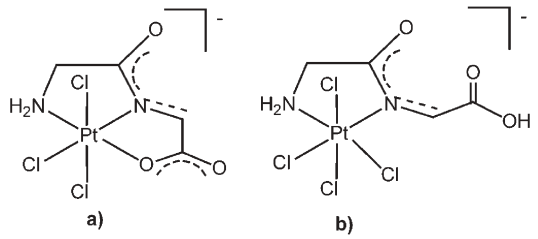

Fig. 20 Structural formulae of (a) $K[Pt(diGly)Cl_3]$ and (b) $K[Pt(HdiGly)Cl_4]$.[74]

Table 7 δ^{195}Pt for a series of Pt(II)/(IV) complexes[74]

	Complex	Donor	δ_{Pt}^{obsd}/ppm
	$K[Pt(diGly)Cl_3]$	Cl_3N_2O	279
	$K[Pt(GlyAla)Cl_3]$	Cl_3N_2O	267
	$K[Pt(AlaGly)Cl_3]$	Cl_3N_2O	247
	$K[Pt(diAla)Cl_3]$	Cl_3N_2O	233
	$K[Pt(HdiGly)Cl_4]$	Cl_4N_2O	−115
	$K[Pt(HGlyAla)Cl_4]$	Cl_4N_2	−107
	$K[Pt(HAlaGly)Cl_4]$	Cl_4N_2	−148
Pt(IV)	$K[Pt(HdiAla)Cl_4]$	Cl_4N_2	−133[b], −143[b]
	$K[Pt(diGly)Cl(OH)_2]$	ClN_2O_3	1270
	$K[Pt(GlyAla)Cl(OH)_2]$	ClN_2O_3	1249
	$K[Pt(AlaGly)Cl(OH)_2]$	ClN_2O_3	1231
	$K[Pt(diAla)Cl(OH)_2]$	ClN_2O_3	1207
	$K[Pt(HdiGly)Cl_2(OH)_2]$	$Cl_2N_2O_2$	899
	$H[Pt(HdiGly)Cl_2(OH)_2]$	$Cl_2N_2O_2$	859
	$K[Pt(HGlyAla)Cl_2(OH)_2]$	$Cl_2N_2O_2$	967
	$K[Pt(HAlaGly)Cl_2(OH)_2]$	$Cl_2N_2O_2$	873
	$K[Pt(HdiAla)Cl_2(OH)_2]$	$Cl_2N_2O_2$	919
	K[Pt(diGly)Cl	ClN_2O	−1870
	K[Pt(GlyAla)Cl]	ClN_2O	−1908
	K[Pt(AlaGly)Cl]	ClN_2O	−1935
Pt(II)	K[Pt(diAla)Cl]	ClN_2O	−1957
	$K[Pt(HdiGly)Cl_2]$	Cl_2N_2	−2140
	$H[Pt(HdiGly)Cl_2]$	Cl_2N_2	−2115
	$K[Pt(HGlyAla)Cl_2]$	Cl_2N_2	−2111
	$K[Pt(HAlaGly)Cl_2]$	Cl_2N_2	−2185

[a] The shifts are relative to Na_2PtCl_6 (the shift for K_2PtCl_4 is −1622 ppm). [b] Postulated to be the D-L-diα-Ala and L-D-diα-Ala stereoisomers.

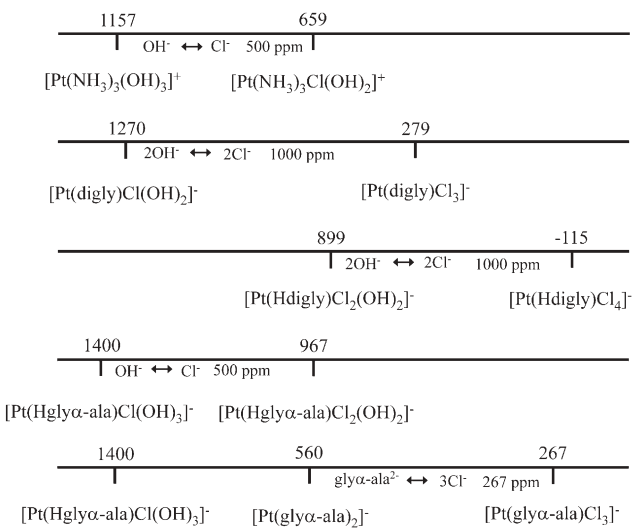

Fig. 21 Relationship between δ^{195}Pt and the structure of Pt(IV) complexes.[74]

4. Coupling constants

4.1 Theoretical studies

Theoretical predictions and calculations of the nuclear spin–spin coupling constants for ^{195}Pt have been limited and reflect the difficulties involved in calculating the relativistic effects of a nucleus with such a large number of electrons (*i.e.*, 78 for ^{195}Pt). General coupling constant theory indicates that the Fermi contact term is the main contributor to J.[19] Ligand-atom spin–spin couplings to ^{195}Pt through one-to-four bonds are well known, however, the theory is more easily developed for one-bond couplings.

The only significant theoretical calculations of J are connected with Pt–Tl compounds and extend to the analysis of $J(^{195}Pt,^{205}Tl)$.[36,37,75] These studies have adopted a relativistic approach and the same models as used by Gilbert and Ziegler[27] for predicting δ^{195}Pt have been used to determine $J(^{195}Pt,^{205}Tl)$.[36,37,75] It was found that the effects from Tl-coordination by the solvent (H_2O) are responsible for half of the magnitude of the large Pt–Tl coupling constant observed.

Münzenberg *et al.*[60] has also found that the *cis*-influence of tertiary phosphorus ligands is characterised by a smaller $^1J(^{31}P,^{195}Pt)$ coupling constant and it has been ascertained that the electron density in the platinum valence orbitals are the dominant parameter in the Fermi contact term that causes the *cis*-influence.

4.2 Experimental studies

^{195}Pt coupling constants are useful for determining the extent of interaction of the platinum centre with coordinated ligands and they also provide valuable information for characterising the geometry of complexes, (for example *cis* and *trans*). In general, the spin–spin interactions vary over several orders of magnitude. For example, $^1J(^1H,^{195}Pt) > 1$ kHz,[76–79] $^1J(^{31}P,^{195}Pt) > 2$ kHz,[18,59,60,77,80–86] $^1J(^{119}Sn,^{195}Pt) > 20$ kHz[68,87,88] (see Fig. 22) and $J(^{195}Pt,^{205}Tl) > 57$ kHz.[36,37,75]

Many examples showing $^nJ(^1H,^{195}Pt)$ have appeared in the literature[3] and there is a large volume of information on platinum couplings with other nuclei. In a series of studies Rochon and coworkers[46,89–93] have reported $^{(1–3)}J$ couplings for ^{195}Pt in a variety of different platinum complexes. Coupling constants are normally visible in ^{1}H,[85,94–101] ^{13}C,[99,102] ^{15}N,[103–105] ^{19}F[77] and ^{31}P[85,106–109] spectra with ^{195}Pt satellites on either side of the NMR signal. As an example, Kumar *et al.*[99] have recorded a one bond ^{13}C–^{1}H correlation (HMQC) spectrum of a platinum–MOP allyl complex in which the ^{195}Pt satellites are clearly seen on either side of the ^{13}C peaks. From this the $^1J(^{13}C,^{195}Pt)$ coupling constant were easily determined (See Fig. 23).[99] Another example demonstrating $J(^{31}P,^{195}Pt)$, $J(^1H,^{31}P)$, $J(^{19}F,^{195}Pt)$ and $J(^1H,^{19}F)$ is shown in Fig. 24.[77]

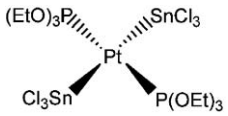

Fig. 22 Pt–Sn complex with large one bond coupling constant of ~ 20 kHz.[16]

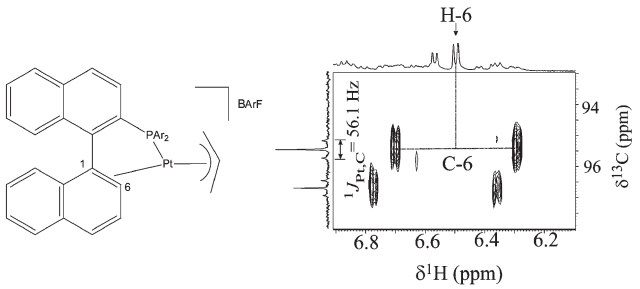

Fig. 23 One bond ^{13}C–^{1}H correlation (HMQC) showing ^{195}Pt satellites and $^{1}J(^{13}C,^{195}Pt)$ coupling for a the platinum–MOP allyl complex (inset) (Ar = substituted phenyl group).[99]

For ^{2}J interactions, such as for ligand–ligand interactions, there is a dependence on the complex configuration (*i.e.*, *cis* or *trans*). Normally the ligands with a *trans* configuration have a larger coupling than with a *cis*-arrangement (*i.e.*, $^{2}J(X,Y)_{trans} >> {}^{2}J(X,Y)_{cis}$ (Fig. 25)). Most platinum–ligand coupling constants have a dependence on the oxidation state of the metal as well as being subject to a *trans*-influence.

^{195}Pt–^{15}N coupling constants are known to be dependent on the s character of the Pt-orbitals used to bind the N-atom.[39,110] The coupling constant values are expected to be smaller for an N-ligand *trans* to a ligand which has a large *trans*-influence since this tends to weaken the bond. For example, in *cis*-$[Pt(NH_3)_2(X)_2]$ complexes the *trans*-influences vary in the order: ligand (^{1}J/Hz) = H_2O (390) < CO_2^- (360) < OH^- (340) < Cl^- (310) < NH_3 (285) < *S*-Met (265). The magnitude of the $J(^{15}N,^{195}Pt)$ coupling constants are Pt–N(peptide) > Pt–N(amine) = Pt–NH_3 (N denotes the deprotonated peptide nitrogen) and the *trans*-influence on Pt–N(amine) or Pt–N(peptide) is >> OH^-, RNH_2, NHY_3 > Cl^-.

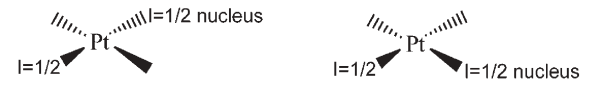

Fig. 25 Square planar Pt complexes with *trans*- (left) and *cis*- (right) spin I = 1/2, or spin-active nuclei

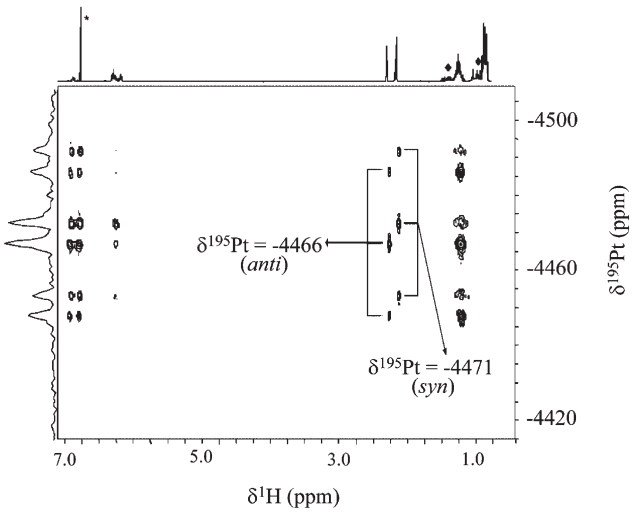

Fig. 26 ^{1}H,^{195}Pt-HMQC spectrum of *cis*-$[Pt(2\text{-}Tol)_2(PEt_3)_2]$. The spectrum shows various long-range correlations between the protons in the 2-Tol and PEt_3 groups and the metal atom. The vertical axis shows the ^{195}Pt signals of both isomers (*syn* and *anti* stereoisomers) as interleaved triplets split by $^{1}J(^{31}P,^{195}Pt)$.[111]

An example of $^{1}J(^{31}P,^{195}Pt)$ coupling constant in *cis*-$[Pt(2\text{-}Tol)_2(PEt_3)_2]$ (2-Tol = 2-toluene) is shown in Fig. 26 where the $^{1}J(^{31}P,^{195}Pt)$ coupling constant were 1751 Hz for the *syn* and

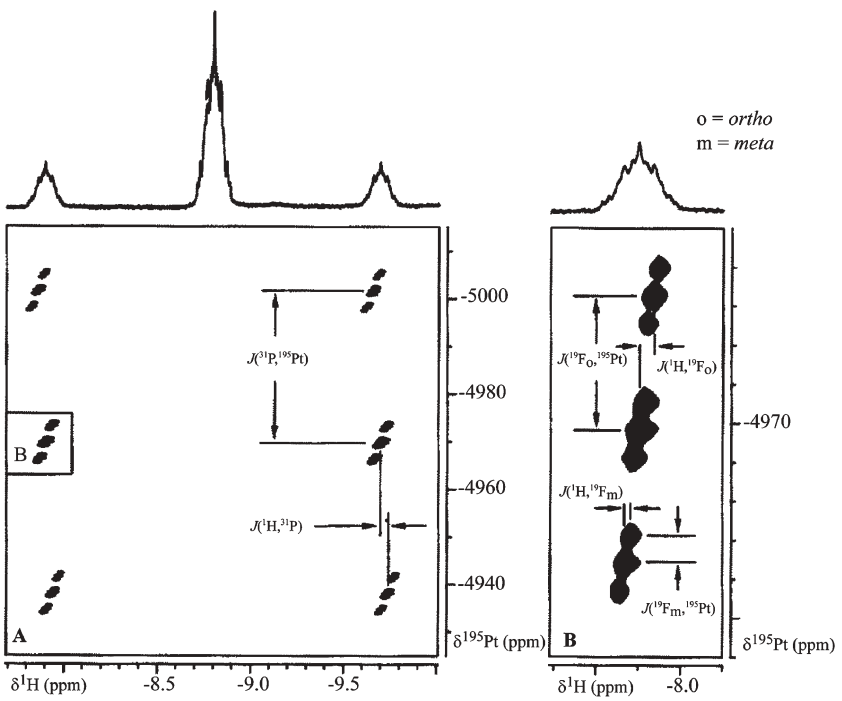

Fig. 24 ^{195}Pt–^{1}H HMQC (9.4 T) for *trans*-$[PtH(C_6F_4CN)(PCy3)_2]$ recorded in $CDCl_3$ showing the multiplicity due to two ^{31}P spins (A) and F_{ortho} and F_{meta} (B). The hydride region of a conventional ^{1}H spectrum is shown above the contour maps.[77]

1739 Hz for the *anti*-configuration.[111] With the possible exception of complexes containing ^{31}P, long range coupling constants such as ^{3}J(spin = 1/2,^{195}Pt) have not received as much attention as ^{1}J(spin = 1/2,^{195}Pt).

It has been documented that the intensity of the satellites due to coupling with ^{195}Pt decreases as the magnetic field of the spectrometer is increased. This is a consequence of the chemical shift anisotropy (CSA) (which will be discussed in Section 5).[98] In conjunction with this a ^{29}Si NMR spectrum with broad ^{195}Pt satellites (marked by arrows) due to the CSA mechanism is shown in Fig. 27.[112] This example shows that the coupling of the metal can extend to three-bonds, or more, and is thus helpful for finding new bonding modes.

An excellent example of the coupling of the ^{19}F nuclei to ^{195}Pt in some fluorinated-platinum complexes is presented in Fig. 28.[113] Also, for the complex *trans*-[PtBr(C_6F_5)(PEt_3)$_2$] (Fig. 29) a ^{5}J(^{19}F, ^{195}Pt) = 18 Hz coupling was measured for the *para* ^{19}F atom.[38]

There are some examples which involve ^{n}J(^{195}Pt–^{195}Pt) couplings mainly in platinum cluster chemistry. Bacheli *et al.*[114] have reported some hydride bridged diplatinum complexes with a ^{2}J(^{195}Pt–^{195}Pt) in the range 250–800 Hz. X-Ray crystallographic studies showed the Pt–Pt distances were in the range of 2.69–2.83 Å confirming the two bond couplings.

Platinum–platinum single-bond formation is a natural consequence of the d^7–d^7 electronic configuration in binuclear complexes, all of which contain two or more bridging ligands.[69] Lippard and coworkers have reported some ^{1}J(^{195}Pt–^{195}Pt) couplings for binuclear Pt(II) and Pt(III) complexes which fall in the range of 600–7000 Hz.[69] They used [Pt_2(en)($C_5H_4NO)_2X_2$]$^{2+}$ (en = ethylenedimane, X = anion) systems to study the influence of the steric interactions on structure and reactivity and thus their influence on metal–metal bonding. Appleton *et al.*[70,115] have reported some platinum aquo complexes involving phosphato bridges with ^{1}J(^{195}Pt–^{195}Pt) couplings of 700–4000 Hz, however complexes with sulfato bridges had larger couplings (1100–5400 Hz). The authors showed that the ^{n}J(^{195}Pt–^{195}Pt) couplings were extremely sensitive to variations in electronic structure but were reasonably insensitive to the molecular structure. In a different study involving platinum amine complexes Appleton *et al.*[103] found a broad singlet and a sharp doublet of doublets with each peak flanked by satellites resulting from Pt–Pt couplings. The authors attributed this J(^{195}Pt–^{195}Pt) = 393 Hz to result from the dinuclear species having non-equivalent Pt nuclei.

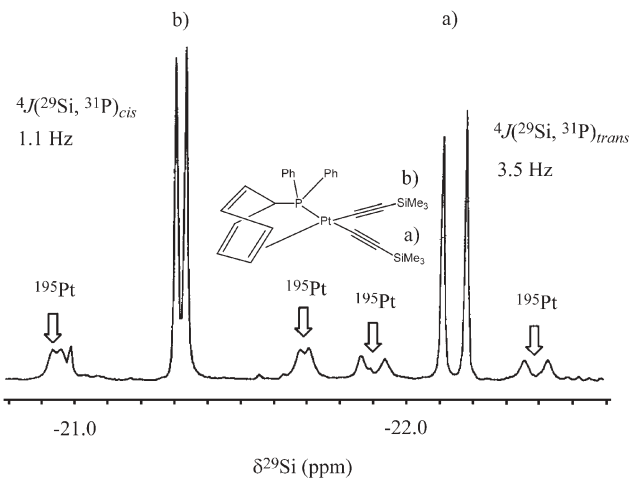

Fig. 27 ^{29}Si (^{1}H decoupled) NMR spectrum of [$Ph_2P(C_7H_7)$]Pt(C≡C-$SiMe_3$)$_2$ in CD_2Cl_2.[112]

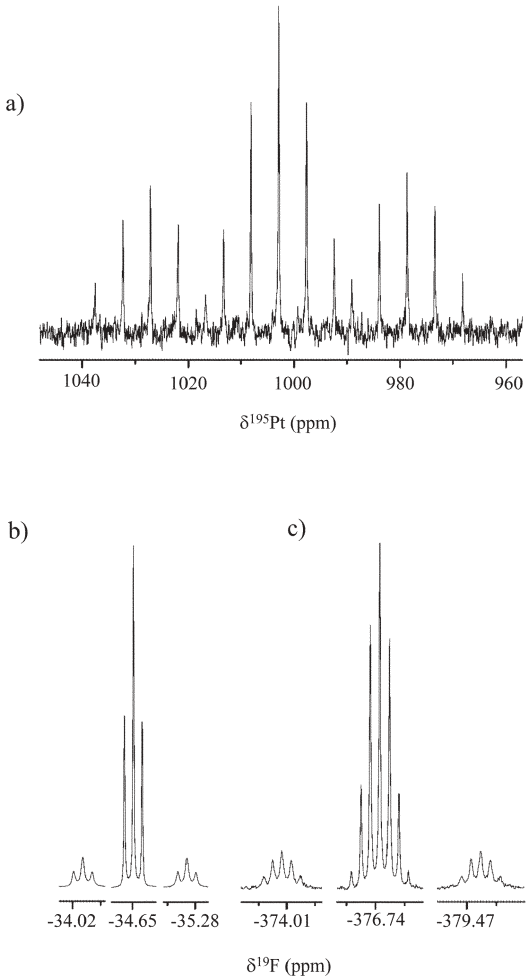

Fig. 28 NMR spectra of $K_2[PtF_2(OD)_2(CF_3)_2]$ in D_2O. (a) ^{195}Pt NMR spectrum (triplet of septets) (b) ^{19}F NMR spectrum of the CF_3 groups (triplet with ^{195}Pt satellites, and (c) ^{19}F NMR spectrum of the metal bound F group (septet with ^{195}Pt satellites).[113]

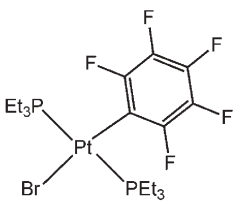

Fig. 29 Structure of *trans*-[PtBr(C_6F_5)(PEt_3)$_2$].[38]

5. Relaxation

NMR relaxation studies provide information on reorientational motion, transport properties, molecular structure and

molecular interactions. The ^{195}Pt spin–lattice (T_1) and spin–spin (T_2) relaxation times fall in the range of 1.7 s to fractions of a second. Spin-rotation and chemical shift anisotropy are the dominant relaxation mechanisms for ^{195}Pt.[3,39]

^{195}Pt nuclei have short T_1 values which allow rapid data acquisition, however, the T_2 values are short and therefore the broad linewidths are sometimes troublesome. Normally the linewidths are $\sim$ 25 Hz for organometallic complexes, however, the value depends on the ligating atoms especially if they have large electric quadrupole moments (for example ^{14}N). The broadening of signals caused by the coupling of quadrupolar nuclei can be removed either by normal or thermal decoupling, the latter taking advantage of the temperature dependence of ^{14}N relaxation.

5.1 Chemical shift anisotropy (CSA)

Chemical shifts are reflections of the local magnetic fields experienced by the observed nuclei. The local fields are different than the applied static field due to the shielding by the local electronic environment. These local fields are anisotropic; consequently, the components of the local fields vary as the molecule reorients due to molecular motion. In solution, the fast reorientational motion results in a single (isotropic) chemical shift, but these varying magnetic fields are a source of relaxation. The maximum CSA for a particular nucleus is of the order of the chemical shift range for the nucleus. Thus ^{195}Pt, which has a large chemical shift range, has a large CSA effect. CSA relaxation increases with the square of the applied field $(B_0)^2$, nuclear screening anisotropy $(\Delta\sigma)^2$, molecular weight and lowering of the temperature (as the reorientational correlation time, τ_c, will be increased).[39]

$$[T_1(\mathrm{Pt})]^{-1}(\mathrm{CSA}) = 6/7[T_2(\mathrm{Pt})]^{-1}(\mathrm{CSA}) = (2/15)\gamma_{\mathrm{Pt}}{}^2 B_0{}^2 \Delta\sigma^2 \tau_c \quad (4)$$

The increase in relaxation rates of the ^{195}Pt nuclei results in broadening of the ^{195}Pt satellites (see Fig. 30). A typical effect of temperature on the linewidths in ^{195}Pt NMR is shown in Fig. 31.

Eqn (4) suggests that Pt-studies can be carried out well at low to intermediate fields (*e.g.*, $\leqslant$ 11.74 T) as CSA effects will be smaller. CSA relaxation of ^{195}Pt can also lead to the

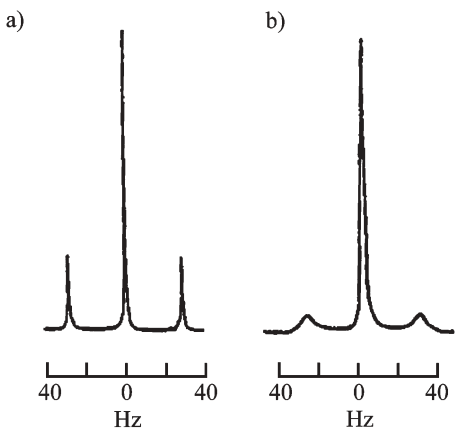

Fig. 30 The ethene ^{1}H NMR resonances of *trans*-[Pt(ethene)(2-carboxy-pyridine)Cl], in $CDCl_3$ at (a) 80 Hz, and (b) 400 MHz.[39]

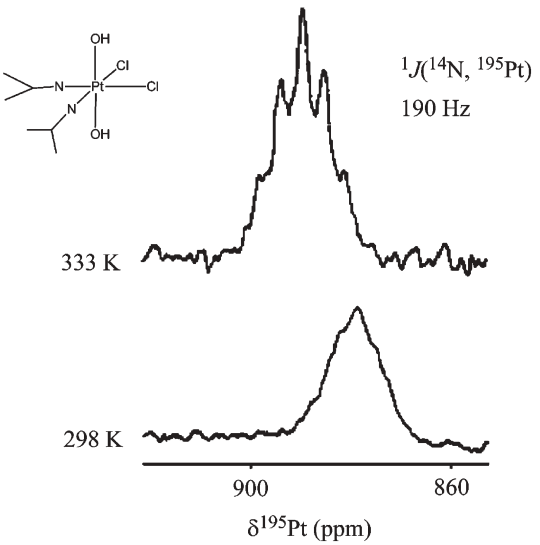

Fig. 31 ^{195}Pt (^{1}H decoupled) NMR spectra of *cis*,*cis*,*trans*-[Pt(isopropylamine)$_2$Cl$_2$(OH)$_2$] in D_2O showing the resolved ^{195}Pt–^{14}N couplings at high temperature (top). Also seen, the temperature dependence of the chemical shift.[39]

disappearance of ^{195}Pt satellites from ^{1}H, ^{13}C, ^{31}P or ^{15}N spectra, which are sometimes useful for detecting binding to macromolecules. The ^{195}Pt satellites appear as 1 : 4 : 1 multiplets and their linewidths are proportional to the spin–lattice relaxation rate of ^{195}Pt, $(2\pi T_1(\mathrm{Pt}))^{-1}$, and therefore, to $B_0{}^2$ as shown above.

5.2 Spin–rotation

Spin–rotation relaxation effects arise from fluctuating magnetic fields generated at the nucleus by the magnetic moment of the molecule. This spin–rotation interaction takes into account the direct interaction between the magnetic fields generated by rapid molecular rotation and the nuclear spins. This relaxation mechanism[3,39,98] is important for small, highly symmetrical complexes, and in contrast to CSA, increases with temperature. The spin–rotation interaction is the dominant relaxation mechanism for $[PtCl_4]^{2-}$ and $[PtCl_6]^{2-}$.[39] The relaxation of the ^{195}Pt nucleus in many phosphorus–platinum compounds has been shown to be governed by CSA and also spin–rotation.[59]

5.3 Experimental studies

^{195}Pt T_1 values of some bi- and tri-metallic species of the form $Cu[PtCl_6]\cdot 6H_2O$ and $Zn_{1-x}Cu_x[PtCl_6]\cdot 6H_2O$ and their temperature dependence are shown in Fig. 32 and 33.[116] In these systems the nuclear relaxation is caused by direct dipolar interaction between the Pt and doped Cu^{2+} ions. A similar temperature dependence was observed for the T_1 values of Pt–Co bimetallic compounds (Fig. 34).[117]

Benn *et al.*[59] have determined the influence of CSA on a series of organoplatinum complexes (with alkene and allyl ligands) by performing T_1 measurements at different magnetic field strengths and various temperatures. In this study chemical shift information was coupled with T_1 values to confirm the different geometries (*i.e.*, *cis* and *trans*) in the

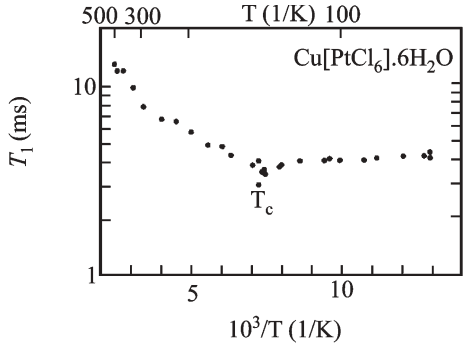

Fig. 32 Temperature dependence of ^{195}Pt T_1 of $Cu[PtCl_6]\cdot 6H_2O$ complex.[116]

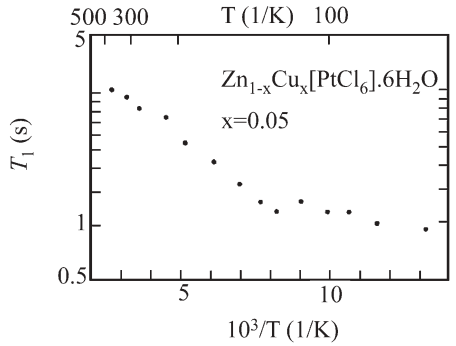

Fig. 33 Temperature dependence of ^{195}Pt T_1 of $Zn_{1-x}Cu_x[PtCl_6]\cdot 6H_2O$ complex.[116]

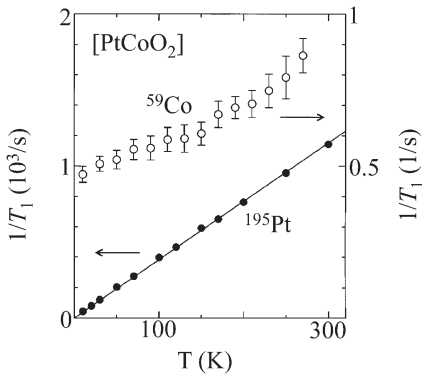

Fig. 34 Temperature dependence of ^{195}Pt and ^{59}Co nuclear spin–lattice relaxation rates ($1/T_1$) in $PtCoO_2$. The solid line is the regression of the relation $(T_1T)^{-1}$ = constant onto the ^{195}Pt data.[117]

Pt–allyl complexes. For the allyl complexes the CSA contributes 50% of the relaxation for both isomers (at 278 K) as compared to the alkene complexes.

Several theoretical advances have also been made in understanding ^{195}Pt relaxation phenomena. For example, Robert and Barra[118] showed the possibility of observing a difference in the high-resolution NMR spectra of two enantiomers and ways to minimise the NMR linewidths of ^{195}Pt resonances. The NMR reorientational correlation equations for dipolar relaxation between ^{1}H and ^{195}Pt have been reported by Carper *et al.*[6] which is applicable when $\omega\tau_c > 1$.

Recently, Yogi *et al.*[119] used ^{195}Pt spin–lattice relaxation measurements to reveal the uniform coexistence of antiferromagnetism and superconductivity in a new alloy of $CePt_3Si$. The authors attribute this strange peculiarity to the lack of an inversion centre in its crystal structure.

6. Applications

6.1 Catalysis and mechanistic studies

^{195}Pt NMR is widely used in chemical research including catalytic and mechanistic studies.[17,111,120–124] Recently, Uccello-Barretta *et al.*[125,126] used chiral Pt(II) complexes as chiral derivatising agents for the enantio-discrimination of unsaturated compounds. δ^{195}Pt, which is sensitive to the charge of a complex,[3] was used to determine the absolute configuration (*R* or *S*) of the chiral product formed. Further, it was shown that ^{195}Pt NMR was helpful in detecting the inequivalences of the diastereoisomeric mixtures arising from the complexation of the metal to the unsaturated carbons.[125,126]

First order rate constants were determined from ^{195}Pt NMR measurements in solutions to study *cis–trans* isomerism of some square-planar platinum(II) nitroimidazole complexes.[127] The reaction mechanism was found to be associative by considering the effects of added halides and the presence of free ligand. In this study information regarding the kinetics of the isomerisation reaction in solution was obtained from the rates of disappearance of the ^{195}Pt peak for the *trans* isomer.

The effect of solvent coordination and ligand changes on the chemical shift[128] of the *cis*- and *trans*-configuration in square planar $[Pt(DMSO)_2(Ar)_2]$, where Ar = Ph, Tol, Mes, Xyl, Me_2Ph, have been studied.[129] δ^{195}Pt and coupling constants (see Table 8) allowed the identification of these configurational isomers and their isomerisation mechanisms.

NMR studies have also been used to identify new bonding modes in several Pd(II) and Pt(II) complexes. Kaminskaia *et al.*[130] have synthesised a new indole complex (Fig. 35) and characterised it using ^{1}H, ^{13}C, ^{15}N and ^{195}Pt NMR. As δ^{195}Pt is sensitive to the type (donor ability) and number of ligating atoms, it is very informative about the composition of the complex, provided the dependence on solvent and temperature is taken into consideration. Referring to the platinum–indole complex shown in Fig. 35, the coupling from the platinum to C(3) was not observed, presumably because of the broadening caused by ^{14}N-induced relaxation. However, broad ^{195}Pt satellites were seen for the hydrogen on C(2) in the ^{1}H NMR spectra and $^{2}J(^{13}C(2),^{195}Pt)$ = 55.8 Hz confirmed a new binding mode.

A similar study involving 1,2-diamine ligands by Martins *et al.*[131] reported a novel non-cisplatin type Pt–acridine complex (Fig. 36). This Pt(II) complex and its analogues were monitored by ^{195}Pt NMR to confirm the $[PtN_2SCl]$ coordination persisted in solution. δ^{195}Pt was ~ -2800 ppm confirming the oxidation state of platinum to be +2.

An extended study on the toxicity and DNA groove binding of platinum nitrogen complexes has been carried out by Wheate *et al.*[132–134] The binding of several dipyrazolylmethane (dpzm) complexes with guanosine and adenosine were characterised using ^{195}Pt NMR. In one study[134] the binding

Table 8 Selected experimental and calculated δ^{195}Pt and coupling constants for the complexes $[Pt(DMSO)_2(Ar)_2]$[129]

	$^3J(^{13}CH_3,^{195}Pt)$ DMSO/Hz	$^1J(^{13}C(1),^{195}Pt)$/Hz	δ^{195}Pt/ppm	Conformation from NMR data	Calcd $^1J(^{13}C(1),^{195}Pt)$/Hz
$[Pt(DMSO)_2(Ph)_2]$	14.9	994.8	−4217	*Cis*	*Cis:* 1018.3 *Trans*: 538.7
$[Pt(DMSO)_2(2\text{-}Tol)_2]$ (*anti*)	13.8, 15.5	1022.3	−4157	*Cis*	*Cis, anti:* 1042.9 *Trans, anti*: 548.1
$[Pt(DMSO)_2(2\text{-}Tol)_2]$ (*syn*)	14.1, 16.0	1021.3	−4165	*Cis*	*Cis, syn:* 1029.2 *Trans, syn*: 536.1
$[Pt(DMSO)_2(3\text{-}Tol)_2]$	14.8	945.5	−4220	*Cis*	*Cis, anti:* 1017.3 *Trans, anti*: 536.1
$[Pt(DMSO)_2(4\text{-}Tol)_2]$	14.9	1002.6	−4212	*Cis*	*Cis:* 1027.5 *Trans*: 541.3
$[Pt(DMSO)_2(Xyl)_2]$	28.8	602.9	−4146	*Trans*	*Cis*: 1139.6 *Trans*: 541.2
$[Pt(DMSO)_2(Mes)_2]$	28.6	605.0	−4148	*Trans*	*Cis*: 1130.4 *Trans*: 546.0
$[Pt(DMSO)_2(Me_5Ph)_2]$	28.5	617.5	−4089	*Trans*	—

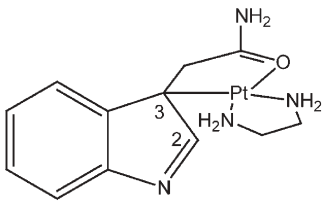

Fig. 35 A new bonding mode in a platinum–indole complex.[130]

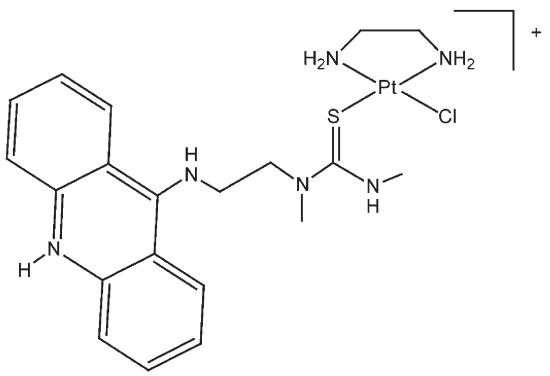

Fig. 36 An analogue of cisplatin type complex.[131]

of guanosine and adenosine to a dinuclear platinum dpzm complex (Fig. 37) caused an upfield shift in the ^{195}Pt resonance from −2338 to −2467 and −2486 ppm, respectively.

In a later study, Wheate *et al.*[135] investigated the binding of cisplatin within cucurbit[7]uril (Q[7]) using ^{195}Pt NMR (Fig. 38). The complexes *cis*-$[PtCl_2(NH_3)_2]$ and *cis*-$[PtCl(NH_3)_2(H_2O)]^+$ were observed at −2160 and −1854 ppm, respectively. The authors suggested that an equilibrium exists between these two species. Upon addition of Q[7] a new ^{195}Pt NMR resonance was observed at −2109 ppm in addition to a shift in the resonance of the aqua form to −1890 ppm. The resonance at −2109 ppm demonstrates total encapsulation within the hydrophobic cavity of Q[7] whereas the resonance at −1890 represents portal binding to the aquated metal complex.

δ^{195}Pt have been reported for chloroplatinate adsorption onto alumina by Shelimov *et al.*[136] (Fig. 39). δ^{195}Pt(IV), which is sensitive to both the first coordination sphere and longer-range effects (solvation sphere), was monitored.

Pellechia *et al.*[137] have followed the time dependence of the Pt(II) complexation with dendrimers using ^{195}Pt NMR

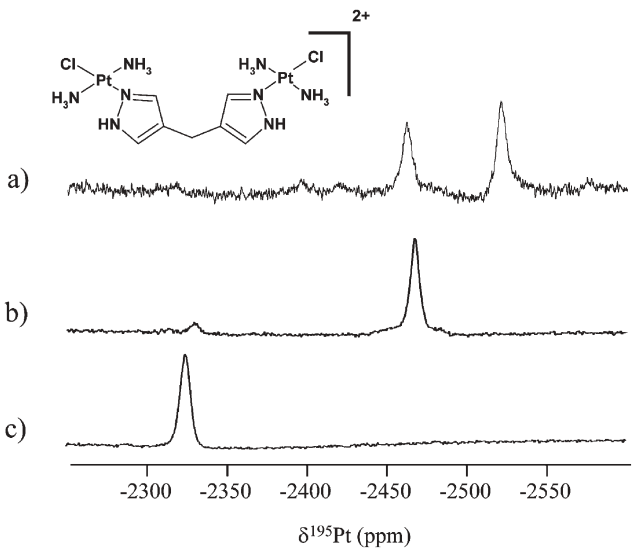

Fig. 37 ^{195}Pt NMR spectra of (a) di-Pt (inset) after reaction with adenosine for 1 week, (b) di-Pt after 24 h reaction with guanosine, and (c) di-Pt.[134]

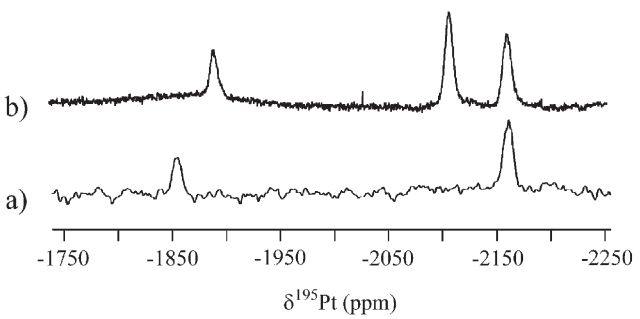

Fig. 38 ^{195}Pt NMR spectra of (a) *cis*-$[Pt(NH_3)_2(H_2O)]$ (−1854 ppm) and *cis*-$[PtCl_2(NH_3)_2]$ (−2160 ppm), and (b) upon addition of Q[7] in D_2O.[135]

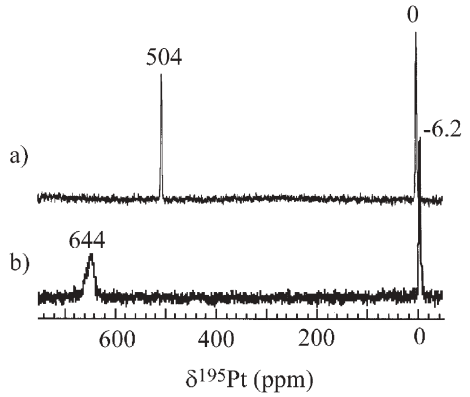

Fig. 39 ^{195}Pt NMR spectra of (a) diluted $[PtCl_6]^{2-}$ and (b) on contact with alumina.[136]

(Fig. 40). The $[PtCl_4]^{2-}$ resonance observed at −1617 ppm decreases in intensity, and the peaks at −1878, −2133 and −2532 ppm increase, indicating that the platinum is bound to one, two and three nitrogen atoms, respectively.

Beni *et al.*[138] have identified a unique hydride complex involving a triangular cluster $[Pt_3(\mu\text{-}CO)(PCy_3)_3(Ph_3Sn)H]$. A non-decoupled ^{195}Pt NMR measurement (see Fig. 41) was carried out to confirm the presence of the hydride ligand. The deduced $^1J(^1H–^{195}Pt)$ coupling constant of 1018 Hz suggested the hydride ligand was coplanar with the metal core.

Abel *et al.*[139] used two dimensional exchange spectroscopy to study the kinetics associated with pyramidal sulfur conversion in the $[PtIMe_3(MeSCH_2CH_2SEt)]$ complex (see Scheme 2 and Fig. 42). The authors were able to find nine distinct rate constants associated with the extensive fluxionality in the platinum(IV) complex.

6.2 Intermetallics

The thermal activation of Pt–Ru fuel cell catalysts has been monitored using ^{195}Pt NMR (including T_1 values)[140] and the authors report similar T_1-values for both Pt-black and their novel Pt–Ru alloy nanoparticle. ^{195}Pt NMR has also been used in the study of semi- and super conductors. For example, Yogi *et al.*[119] have reported a new antiferromagnetic heavy-fermion superconductor $CePt_3Si$ without an inversion centre. Another study by Tou *et al.*[141] investigated UPt_3 and UNi_2Al_3 heavy-fermion superconductors. Recently Ma *et al.*[142] have

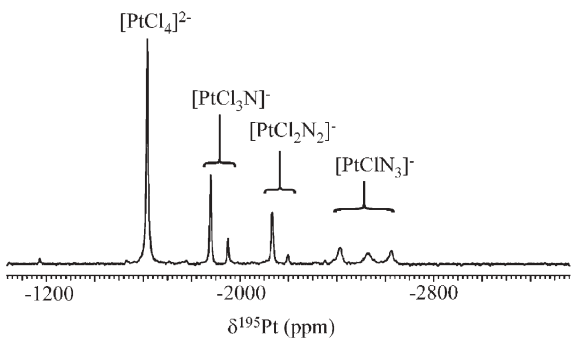

Fig. 40 ^{195}Pt NMR spectrum of the complex formed between 0.09 M $K_2[PtCl_4]$ and 0.009 M dendrimer in 9.1% D_2O solution.[137]

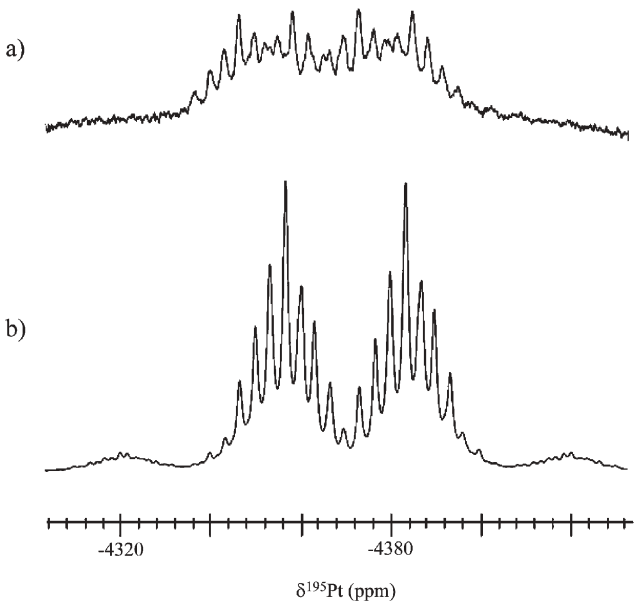

Fig. 41 Hydride indication from (a) non-decoupled and (b) ^{1}H decoupled ^{195}Pt NMR spectra of $[Pt_3(\mu\text{-}CO)(PCy3)_3(Ph_3Sn)H]$ in CD_2Cl_2.[138]

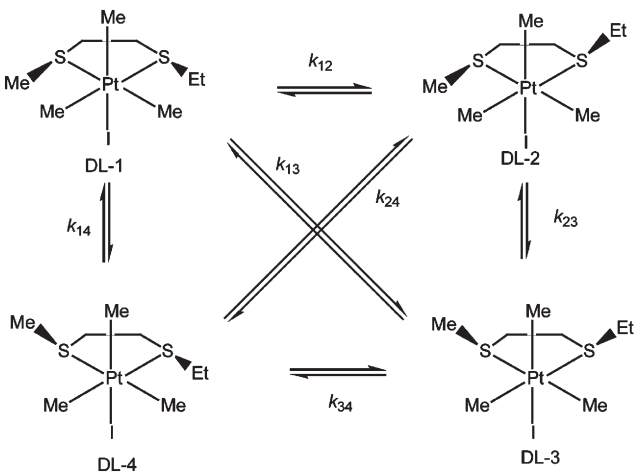

Scheme 2 The four isomers of $[PtIMe_3(MeSCH_2CH_2SEt)]$ showing different sulfur inversion pathways.[139]

synthesised novel porphyrin–thallium–platinum complexes with a "naked" metal–metal bond. ^{195}Pt and ^{205}Tl NMR confirmed the metal–metal bond. This bond results in a very strong one-bond ^{195}Pt–^{205}Tl spin–spin coupling of 47.8 and 48.3 kHz for two different porphyrin complexes (Fig. 43).

6.3 Pharmaceutical chemistry (drug binding studies)

^{195}Pt NMR is playing a major role in pharmaceutical chemistry especially in the development of Pt-containing anti-tumour drugs (for example, cisplatin and carboplatin).[143] The anti-tumour activity of these drugs is believed to result from the strong bonding of the platinum to DNA and many kinds of DNA adducts have been identified.[23,24,144,145] ^{195}Pt NMR has helped to clarify protein recognition of platinated DNA and the design of sequence-specific DNA-binding drugs.

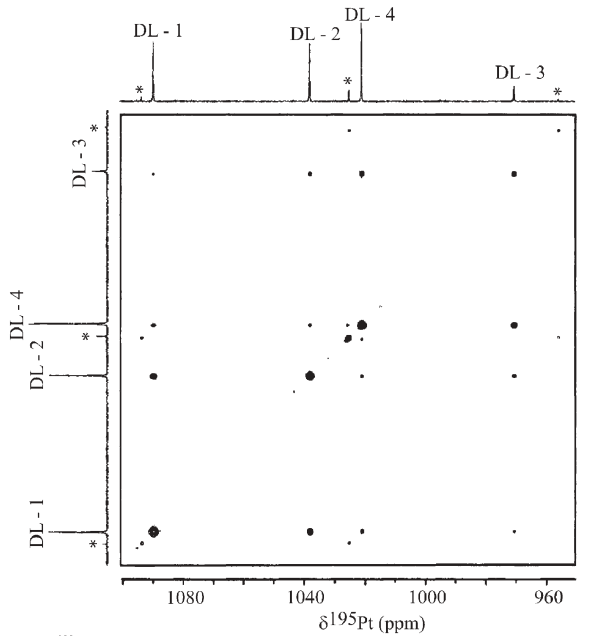

Fig. 42 ^{195}Pt 2D exchange spectrum of $[PtIMe_3(MeSCH_2CH_2SEt)]$ ($CDCl_3$ solution, 263 K, τ_m = 0.08 s). Signals (marked *) are due to a small amount of $[PtIMe_3(MeSCH_2CH_2SMe)]$.[139]

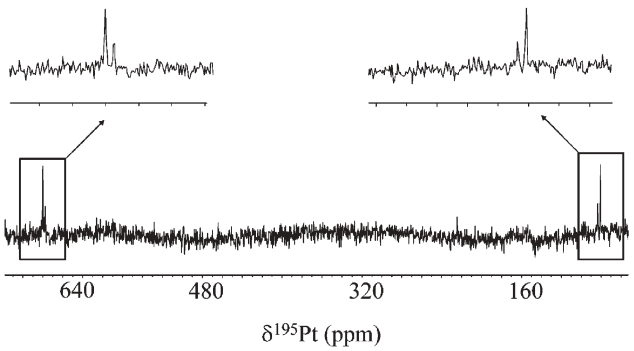

Fig. 43 ^{195}Pt NMR spectrum of $[(NC)_5Pt–Tl(tpp)]^{2-}$ in DMSO–THF–CH_2Cl_2 (1 : 1 : 1 volume ratio) solution at 298 K (lower trace) and expanded doublet signals (upper).[142]

Several authors have reviewed the application of ^{195}Pt NMR in pharmaceutical chemistry.[24,39,45] Representative δ^{195}Pt for anti-tumour and related complexes are given in Table 9.[39]

Traditional NMR binding studies have been conducted by observing changes in chemical shifts and intensities of resonances during a time course of 1D ^{195}Pt NMR experiments.[7,146–148] For example, the preferred binding site of cisplatin to DNA is the N7 of guanine[149] and binding involves successive displacement of Cl^- by the purine N, thus leading to low frequency shifts in the ^{195}Pt NMR spectrum. Using a time course of single pulse 1D NMR experiments several groups[7,150,151] have monitored the formation and closure of adducts during the course of DNA binding reactions. *trans*-Monofunctional adducts appear to react more rapidly with glutathione than those of *cis* isomers suggesting that selective trapping of transplatin monofunctional adducts *in vivo* could contribute to the biological inactivity of the *trans* isomer.[64,150,152] Recently, Jansen *et al.*[153] used ^{195}Pt NMR to identify reaction intermediates and products of several variations of cisplatin. They found that *cis*-$[PtCl_2X_2]$ ($X=NH_2C(CH_2CH_2COOH)_3)_2$ is unable to bind to DNA, whereas *cis*-$[PtCl_2X(NH_3)]$ binds only to one nucleotide.

The kinetics and mechanism of cisplatin and transplatin binding to DNA including the determination of the lifetimes of monofunctional adducts was studied using ^{195}Pt NMR.[7] The evolution of the species formed during platination reactions was followed and the rate determining steps in the formation and closure of the monofunctional adducts elucidated. The results indicated that the steady-state concentrations of aquated species formed during the reaction of cisplatin with DNA are very low, explaining why they were not observed in the ^{195}Pt NMR spectra. As cisplatin is consumed, new resonances appear at ~150–220 ppm and 300–350 ppm upfield of the cisplatin resonance (see Fig. 44). The chemical shifts of these resonances were consistent with the presence of mono- and bifunctional adducts (*vide infra*).

The effect of cisplatin on tubulin polymerisation has been studied *in vitro*.[154] Dynamic ^{195}Pt NMR spectra of tubulin-containing solutions of *cis*-$[Pt(NH_3)_2(H_2O)_2]^{2+}$ were recorded. The experiments revealed that cisplatin stops tubulin assembly, helping to uncover the molecular mechanisms of antitumor activity of platinum complexes.

The systematic pattern of substitution effects of NH_3–H_2O in Pt(II) complexes is illustrated in Fig. 45 which shows the sensitivity of the δ^{195}Pt to changes in the bound ligands thus being useful in the characterisation of new drugs.[39] The

Table 9 δ^{15}N, δ^{195}Pt and one-bond coupling constants for Pt(II) and Pt(IV) diamines[39]

	Complex	δ^{195}Pt/ppm	δ^{15}N/ppm	$^1J(^{15}N,^{195}Pt)$/Hz	Solvent
Pt(IV)	*Cis*, *trans*-$[Pt(NH_3)_2(mal)(OH)_2]$	1570	—	—	D_2O–H_2O_2
	Cis-$[Pt(C_3H_7NH_2)_2(OH)_4]$	1521	—	249	D_2O
	Cis, *cis*, *trans*-$[Pt(C_3H_7NH_2)_2Cl_2(OH)_2]$	881	—	266	D_2O
	Cis, *cis*, *trans*-$[Pt(NH_3)_2Cl_2(OH)_2]$	860	−37.9	275	H_2O–H_2O_2
	Cis-$[Pt(NH_3)_2Cl_4]$	−145	−30.5	247	H_2O
Pt(II)	$[Pt(NH_3)_2(OH)]_2^{2+}$	—	−81.7	342	H_2O
	$[Pt(NH_3)_2(OH)]_2^{3+}$	−1499	−79.1	339	H_2O
	Cis-$[Pt(NH_3)_2(H_2O)]_2^{2+}$	−1590	−89.0	387	H_2O
	$[Pt(NH_3)_2(Etmal)]$	−1694	−83.7	366	H_2O
	$[Pt(NH_3)_2(CBDCA)]$	−1723	—	360	H_2O
	$[Pt(en)(H_2O)]_2^{2+}$	−1914	−51.9	411	H_2O
	Cis-$[Pt(NH_3)_2Cl_2]$	−2048	—	302	DMF
		−2097	—	312	DMSO
		−2168	—	312	H_2O

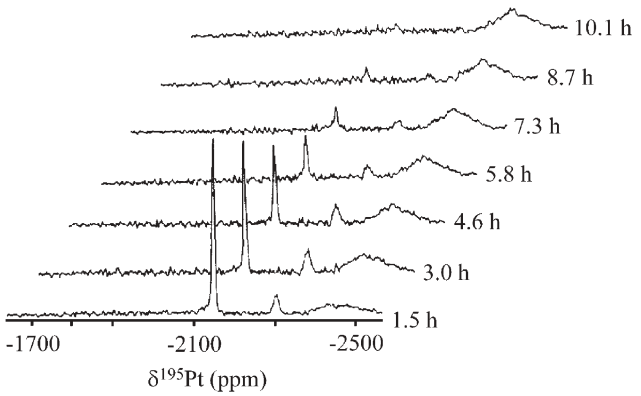

Fig. 44 Time dependent ^{195}Pt NMR spectra of the reaction between cisplatin and chicken-erythrocyte DNA at 37 °C.[7]

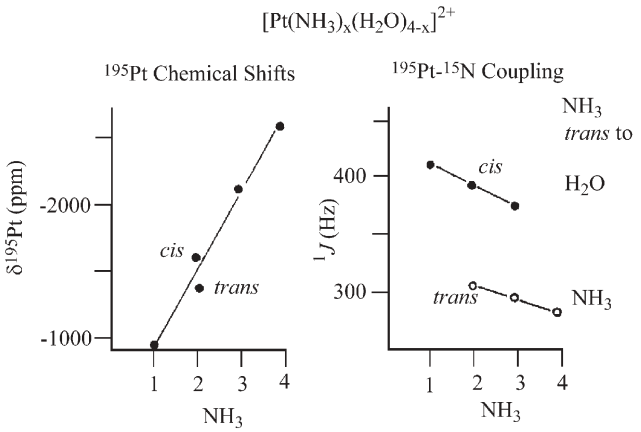

Fig. 45 Plots of the variation in δ^{195}Pt (left) and ^{195}Pt-$^{-15}$N one-bond coupling constants (right) with the number of NH_3 ligands in $[Pt(NH_3)_x(H_2O)_{4-x}]^{2+}$.[39]

interaction of a 1 : 1 solution of *cis*-[Pt($^{15}NH_3$)$_2$Cl$_2$] and inosine with nucleic acid bases has been studied using ^{195}Pt NMR. The broadening of the ^{195}Pt resonances suggests the interaction of inosine (*via* ^{14}N) with the Pt-complex (see Fig. 46).

The solution chemistry of *trans*-diammineplatinum(II) complexes in relation to anticancer activity have been studied.[30,155] ^{195}Pt NMR spectra have been used to characterise in solution *trans*-diammineplatinum(II) complexes with aqua, chloro, nitrato, sulfato, acetate, and phosphate ligands.[49,50]

A recent study involving the monitoring of local disposition kinetics of carboplatin after subcutaneous injection in rats was studied using ^{195}Pt NMR.[156] The *in vitro* measurements were performed in different solvents containing potassium tetrachloroplatinate(II), carboplatin and cisplatin which showed resonances at −1623, −1705 and −2060 ppm, respectively. The T_1 relaxation time of carboplatin was found to be around 100 ms. *In vivo* measurement, however, for carboplatin in rats showed a broad resonance at δ = −1715 ppm, thus confirming the local disposition kinetics.

An extensive study of the Pt(II) and Pt(IV) monoadducts of the type [Pt(DACH)(L)Cl]NO$_3$ and [Pt(DACH)*trans*-(X)$_2$(L)Cl]NO$_3$ (DACH = *trans*-diaminocyclohexane)

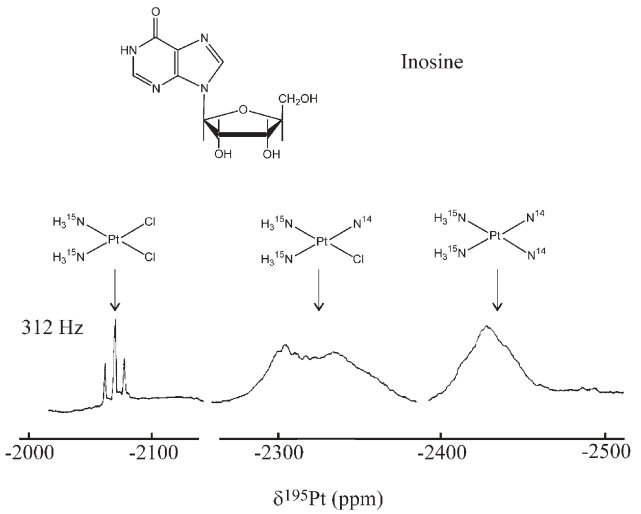

Fig. 46 ^{195}Pt (^{1}H decoupled) NMR spectrum of a 1 : 1 solution of *cis*-[Pt($^{15}NH_3$)$_2$Cl$_2$] and inosine (50 mM) in 90%–10% H_2O–D_2O.[39]

complexes has been carried out by Ali *et al.*[157] where L = adenine, guanine, hypoxanthine, cytosine, adenosine, guanosine, inosine, cytidine, 9-ethylguanine or 1-methylcytosine. All complexes were characterised by ^{195}Pt NMR. δ^{195}Pt has also been recorded for other complexes with the DACH ligand[158,159] and are summarised in Table 10.

7. Advanced NMR techniques

This section extends the applications of ^{195}Pt NMR to solid-state, imaging and other novel techniques. The first example of the use of ^{195}Pt PGSE diffusion NMR appeared in 2005 and was used to observe the solvent dependence of aggregation of the hexachloroplatinate dianion in $Na_2[PtCl_6]$ and $H_2[PtCl_6]$.[12] The ^{195}Pt PGSE method[160,161] was able to distinguish the different aggregation states in water and methanol.

Siegel *et al.*[162] have carried out solid-state ^{195}Pt NMR experiments using a Carr-Purcell Meiboom-Gill (CPMG) sequence on the square-planar [Pt(PPh$_3$)$_2$(C$_2$H$_4$)] (Fig. 47) and [Pt(PEt$_3$)$_2$(OCO)$_2$]·xH$_2$O (Fig. 48) complexes. The heavy ^{195}Pt nuclei exhibit chemical shifts that range over 1000 ppm, depending on the orientation of the molecule with respect to the static magnetic field.

Grykalowska and Nowak[163] have reported ^{195}Pt-MAS (magic-angle spinning) NMR on a series of MPtSn (M = Ti, Zr, Hf, Th) complexes (Fig. 49) used in semiconductor technology.

Multinuclear magnetic resonance imaging has been used to monitor the transport of a γ-Al_2O_3 pellet in an aqueous solution of $H_2[PtCl_6]$ (see Fig. 50).[164] ^{195}Pt NMR, in conjunction with ^{1}H and ^{31}P, has been shown to be useful for non-invasive visualisation of the preparation of catalysts and other supported materials.

8. Closing remarks and future prospects

With the availability of magnetic fields reaching the giga-Hertz range and the accessibility of higher magnetic gradient strengths, ^{195}Pt NMR has expanded rapidly in recent years.

Table 10 δ^{195}Pt for selected platinum complexes in D_2O[157]

	Complex	δ^{195}Pt/ppm
Adenine	[Pt(DACH)(Ade)Cl]NO_3	−2537
	[Pt(DACH)*trans*-$(OH)_2$(Ade)Cl]$NO_3\cdot H_2O$	633
	[Pt(DACH)*trans*-(acetate)$_2$(Ade)Cl]NO_3	841
Guanine	[Pt(DACH)(Gua)Cl]NO_3	−2519
	[Pt(DACH)*trans*-$(OH)_2$(Gua)Cl]$NO_3\cdot H_2O$	640
	[Pt(DACH)*trans*-(acetate)$_2$(Gua)Cl]$NO_3\cdot 2H_2O$	850
Hypoxanthine	[Pt(DACH)(Hyp)Cl]NO_3	−2515
	[Pt(DACH)*trans*-$(OH)_2$(Hyp)Cl]$NO_3\cdot H_2O$	650
	[Pt(DACH)*trans*-(acetate)$_2$(Hyp)Cl]$NO_3\cdot 2H_2O$	870
Cytosine	[Pt(DACH)(Cyt)Cl]NO_3	−2549
	[Pt(DACH)*trans*-$(OH)_2$(Cyt)Cl]$NO_3\cdot H_2O$	674
	[Pt(DACH)*trans*-(acetate)$_2$(Cyt)Cl]$NO_3\cdot H_2O$	875
Adenosine	[Pt(DACH)(Ado)Cl]NO_3	−2579
	[Pt(DACH)*trans*-$(OH)_2$(Ado)Cl]$NO_3\cdot 2H_2O$	649
	[Pt(DACH)*trans*-(acetate)$_2$(Ado)Cl]$NO_3\cdot 2H_2O$	845
Guanosine	[Pt(DACH)(Guo)Cl]NO_3	−2519
	[Pt(DACH)*trans*-$(OH)_2$(Guo)Cl]$NO_3\cdot H_2O$	566
	[Pt(DACH)*trans*-(acetate)$_2$(Guo)Cl]$NO_3\cdot 2H_2O$	778
Inosine	[Pt(DACH)(Ino)Cl]NO_3	−2519
	[Pt(DACH)*trans*-$(OH)_2$(Ino)Cl]NO_3	563
	[Pt(DACH)*trans*-(acetate)$_2$(Ino)Cl]$NO_3\cdot 2H_2O$	849
Cytidine	[Pt(DACH)(Cyd)Cl]NO_3	−2537
	[Pt(DACH)*trans*-$(OH)_2$(Cyd)Cl]NO_3	660
	[Pt(DACH)*trans*-(acetate)$_2$(Cyd)Cl]$NO_3\cdot 2H_2O$	739
9-Ethylguanine	[Pt(DACH)(9-EtGua)Cl]NO_3	−2514
	[Pt(DACH)*trans*-$(OH)_2$(9-EtGua)Cl]$NO_3\cdot 2H_2O$	578
	[Pt(DACH)*trans*-(acetate)$_2$(9-EtGua)Cl]$NO_3\cdot 2H_2O$	841
1-Methylcytosine	[Pt(DACH)(1-MeCyt)Cl]NO_3	−2545
	[Pt(DACH)*trans*-$(OH)_2$(1-MeCyt)Cl]$NO_3\cdot 2H_2O$	784
	[Pt(DACH)*trans*-(acetate)$_2$(1-MeCyt)Cl]$NO_3\cdot 2H_2O$	862
	[Pt(*S,S*-DACH)(5-Cl-Phen)]$^{2+}$	−2828[a]
	[Pt(*R,R*-DACH)(5-Cl-Phen)]$^{2+}$	−2837[a]
	[Pt(*S,S*-DACH)(5-Me-Phen)]$^{2+}$	−2807[a]
	[Pt(*S,S*-DACH)(5-NH_2-Phen)]$^{2+}$	−2798[a]

[a] From ref. 159

Novel methods have been developed to get fast, efficient and accurate predictions of chemical shifts and coupling constants with a myriad of applications including the detection of new bonding modes, the study of intermetallics and the identification of intermediates in reaction mechanisms. With the synthesis of new platinum compounds daily and the available NMR knowledge expanding rapidly, the possibilities of using ^{195}Pt NMR are becoming unlimited. In particular, ^{195}Pt NMR has become a valuable tool in pharmaceutical and drug binding studies for explaining the unprecedented biological and chemical processes of some new drugs. The unparalleled growth in the solid-state NMR and imaging techniques can be envisaged to further applications as well.

In the final stages of preparation of this article the authors have noted that a new review article on ^{195}Pt NMR has just been published by Rochon and coworkers.[93]

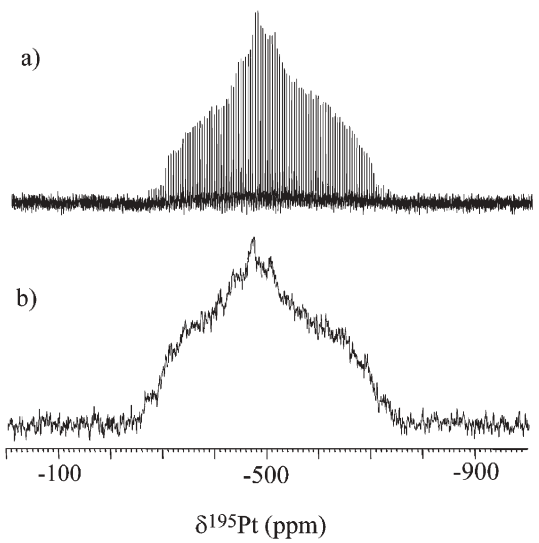

Fig. 47 ^{195}Pt solid-state NMR spectra of [Pt$(PPh_3)_2(C_2H_4)$] (a) cross polarisation-CPMG spectrum and (b) spin-echo CPMG spectrum.[162]

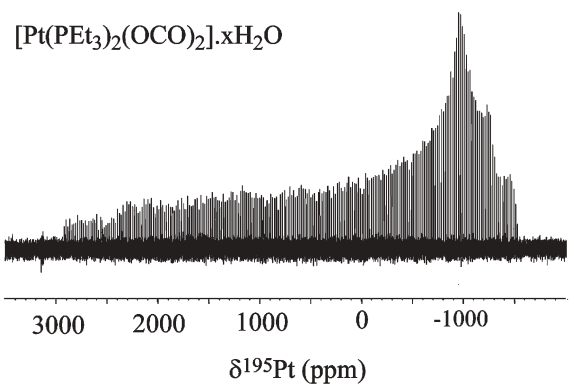

Fig. 48 ^{195}Pt solid-state NMR spectrum obtained using a modified CPMG pulse sequence.[162]

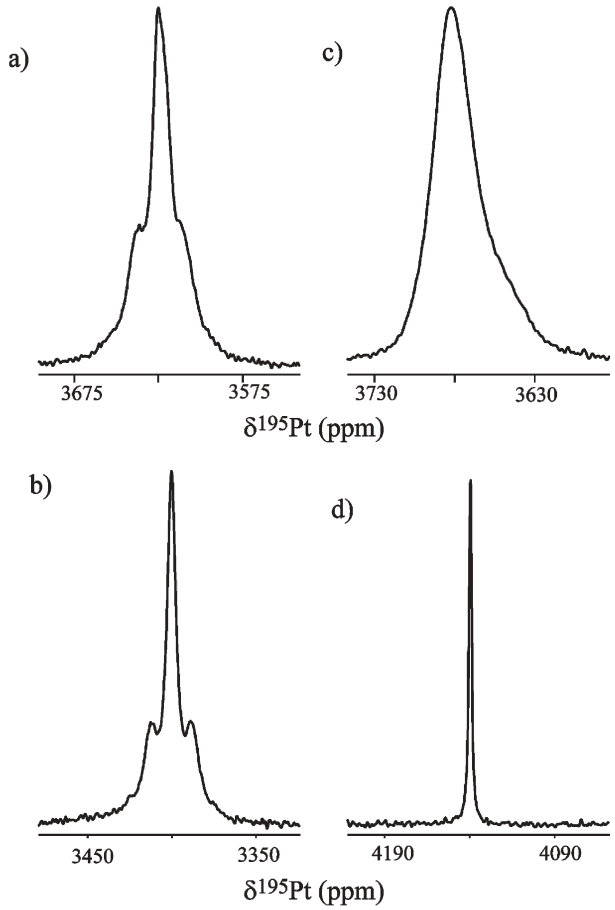

Fig. 49 ^{195}Pt MAS NMR spectra of (a) TiPtSn, (b) ZrPtSn, (c) HfPtSn and (d) ThPtSn. The spinning rates were 8.0, 6.5, 9.3 and 6.5 kHz, respectively.[163]

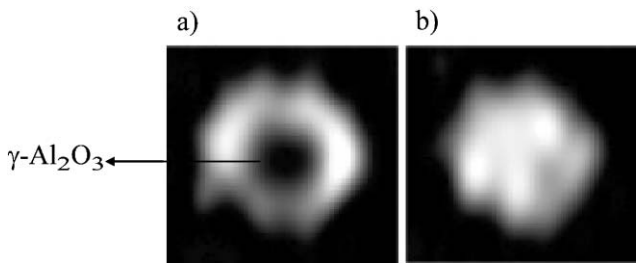

Fig. 50 ^{195}Pt NMR images of the impregnation of an γ-Al_2O_3 pellet with an aqueous solution of $H_2[PtCl_6]$ at (a) 14 min and (b) 70 min after pellet immersion.[164]

Acknowledgements

The NSW State Government is acknowledged for support through a BioFirst award to WSP. BMS thanks the Australian government and the University of Western Sydney for support through an Honours scholarship and an Australian Postgraduate Award scholarship and Dr Nial Wheate is thanked for useful comments.

References

1 A. V. Zelewsky, *Helv. Chim. Acta*, 1968, **51**, 803.
2 A. Pidcock, R. E. Richards and L. M. Venanzi, *J. Chem. Soc. A*, 1968, 1970.
3 P. S. Pregosin, *Coord. Chem. Rev.*, 1982, **44**, 247.
4 J. G. Collins, A. D. Sleeman, J. R. Aldrich-Wright, I. Greguric and T. W. Hambley, *Inorg. Chem.*, 1998, **37**, 3133.
5 B. E. Schwederski, H. D. Lee and D. W. Margerum, *Inorg. Chem.*, 1990, **29**, 3569.
6 W. R. Carper, Z. Meng and N. M. Palko, *J. Mol. Liq.*, 2002, **98**, 7.
7 D. P. Bancroft, C. A. Lepre and S. J. Lippard, *J. Am. Chem. Soc.*, 1990, **112**, 6860.
8 J. R. Aldrich-Wright, C. Brodie, E. C. Glazer, N. W. Luedtke, L. Elson-Schwab and Y. Tor, *Chem. Commun.*, 2004, 1018.
9 J. R. Aldrich-Wright, R. F. Fenton, I. D. Greguric, T. W. Hambley and P. A. Williams, *J. Chem. Soc., Dalton Trans.*, 2002, 4666.
10 R. R. Fenton and J. R. Aldrich-Wright, in *Metal Complexes and Therapeutic uses thereof*, International Patent, 2002.
11 W. S. Price, *Aust. J. Chem.*, 2003, **56**, 855.
12 D. Nama, P. G. A. Kumar and P. S. Pregosin, *Magn. Reson. Chem.*, 2005, **43**, 246.
13 T. D. W. Claridge, *High Resolution NMR Techniques in Organic Chemistry*, Elsevier, Oxford, UK, 1999, pp. 222, 226 and 229.
14 P. Granger and R. K. Harris, in *Multinuclear Magnetic Resonance in Liquids and Solids - Chemical Applications*, Kluwer Academic Publishers, Dordrecht, The Netherlands, 1990.
15 M. H. Levitt, *Spin Dynamics - Basics of Nuclear Magnetic Resonance*, Wiley, Chichester, UK, 2001.
16 P. S. Pregosin and H. Rüegger, Nuclear Magnetic Resonance Spectroscopy in *Comprehensive Coordination Chemistry II*, ed. J. A. McCleverty and T. J. Meyer, Elsevier, Amsterdam, The Netherlands, 2003, pp. 1–35.
17 D. Gudat, A. Dogan, W. Kaim and A. Klein, *Magn. Reson. Chem.*, 2004, **42**, 781.
18 H. Rüegger and D. Moskau, *Magn. Reson. Chem.*, 1991, **29**, S11.
19 P. Pyykkö, *Theor. Chem. Acc.*, 2000, **103**, 214.
20 C. Benzi, O. Crescenzi, M. Pavone and V. Barone, *Magn. Reson. Chem.*, 2004, **42**, S57.
21 R. C. Mawhinney and G. Schreckenbach, *Magn. Reson. Chem.*, 2004, **42**, S88.
22 N. F. Ramsey, *Phys. Rev.*, 1950, **78**, 699.
23 S. J. Berners-Price and P. J. Sadler, *Coord. Chem. Rev.*, 1996, **151**, 1.
24 B. Rosenberg, P. J. O'Dwyer, J. P. Stevenson, A. Eastman, S. W. Johnson, D. B. Zamble, S. J. Lippard, Y. Chen, Z. Guo and P. J. Sadler, 'Cisplatin: Chemistry and Biochemistry of a Leading Anticancer Drug', ed. B. Lippert, Wiley, 1999.
25 N. F. Ramsey, *Phys. Rev.*, 1950, **77**, 567.
26 G. Schreckenbach and T. Ziegler, *Int. J. Quantum Chem.*, 1997, **61**, 899.
27 T. M. Gilbert and T. Ziegler, *J. Phys. Chem. A*, 1999, **103**, 7535.
28 R. R. Dean and J. C. Green, *J. Chem. Soc. A*, 1968, 3047.
29 P. L. Goggin, R. J. Goodfellow, S. R. Haddock, B. F. Taylor and F. R. H. Marshall, *J. Chem. Soc., Dalton Trans.*, 1976, 459.
30 T. G. Appleton, J. R. Hall and S. F. Ralph, *Inorg. Chem.*, 1985, **24**, 4685.
31 Y. Koie, S. Shinode and Y. Saito, *J. Chem. Soc., Dalton Trans.*, 1981, 1082.
32 S. K. Wolff, T. Ziegler, E. van Lenthe and E. J. Baerends, *J. Chem. Phys.*, 1999, **110**, 7689.
33 J. G. Snijders, E. J. Baerends and P. Ros, *Mol. Phys.*, 1979, **38**, 1909.
34 E. Penka Fowe, P. Belser, C. Daul and H. Chermette, *Phys. Chem. Chem. Phys.*, 2005, **7**, 1732.
35 B. Le Guennic, K. Matsumoto and J. Autschbach, *Magn. Reson. Chem.*, 2004, **42**, S99.
36 J. Autschbach and B. Le Guennic, *J. Am. Chem. Soc.*, 2003, **125**, 13585.
37 J. Autschbach and B. Le Guennic, *Chem.–Eur. J.*, 2004, **10**, 2581.
38 P. S. Pregosin, 'Transition Metal Nuclear Magnetic Resonance', Elsevier, Amsterdam, The Netherlands, 1991.
39 I. M. Ismail and P. J. Sadler, in ^{195}Pt and ^{15}N NMR Studies of Antitumour Complexes, *ACS Symposium Series 'Platinum Gold, and Other Metal Chemotherapeutic Agents'*, Univ. London, London, UK, 1983, pp. 171–190.
40 P. S. Pregosin and H. Rüegger, *Inorg. Chim. Acta*, 1984, **86**, 55.
41 R. Colton and V. Tedesco, *Inorg. Chim. Acta*, 1992, **202**, 95.

42 F. Asaro, M. Lenarda, G. Pellizer and L. Storaro, *Spectrochim. Acta, Part A*, 2000, **56**, 2167.
43 L. G. Marzilli, Y. Hayden and M. D. Reily, *Inorg. Chem.*, 1986, **25**, 974.
44 P. Dotta, P. G. A. Kumar and P. S. Pregosin, *Helv. Chim. Acta*, 2004, **87**, 272.
45 K. J. Barnham, S. J. Berners-Price, Z. Guo, P. D. S. Murdoch and P. J. Sadler, NMR Spectroscopy of Platinum Drugs: From DNA to Body Fluids, in *Platinum and other metal coordination compounds in cancer chemotherapy 2*, ed. S. van de Velde and J. H. Schornagel, Plenum Press, New York, USA, 1996, pp. 1–17.
46 F. D. Rochon and V. Buculei, *Inorg. Chim. Acta*, 2005, **358**, 3919.
47 F. D. Rochon and V. Buculei, *Inorg. Chim. Acta*, 2005, **358**, 2040.
48 F. D. Rochon and V. Buculei, *Inorg. Chim. Acta*, 2004, **357**, 2218.
49 T. G. Appleton, R. D. Berry, C. A. Davis, J. R. Hall and H. A. Kimlin, *Inorg. Chem.*, 1984, **23**, 3514.
50 T. G. Appleton, J. R. Hall, S. F. Ralph and C. S. M. Thompson, *Inorg. Chem.*, 1984, **23**, 3521.
51 N. P. Farrell, *Transition Metal Complexes as Drug and Chemotherapeutic Agents*, Kluwer Academic Publishers, Dordrecht, The Netherlands, 1989.
52 N. P. Farrell and Y. Qu, *Inorg. Chem.*, 1989, **28**, 3416.
53 N. P. Farrell, Y. Qu and M. P. Hacker, *J. Med. Chem.*, 1990, **33**, 2179.
54 N. P. Farrell, S. G. Dealmeida and K. A. Skov, *J. Am. Chem. Soc.*, 1988, **110**, 5018.
55 Y. Qu, T. G. Appleton, J. D. Hoeschele and N. Farrell, *Inorg. Chem.*, 1993, **32**, 2591.
56 Y. Qu, S. G. Dealmeida and N. Farrell, *Inorg. Chim. Acta*, 1992, **201**, 123.
57 Y. Qu and N. Farrell, *Inorg. Chem.*, 1992, **31**, 930.
58 Y. Qu, H. Rauter, A. P. S. Fontes, R. Bandarage, L. R. Kelland and N. Farrell, *J. Med. Chem.*, 2000, **43**, 3189.
59 R. Benn, R.-D. Reinhart and A. Rufińska, *J. Organomet. Chem.*, 1985, **282**, 291.
60 R. Münzenberg, P. Rademacher and R. Boese, *J. Mol. Struct.*, 1998, **444**, 77.
61 S. J. Berners-Price, T. G. Appleton, V. Brabec, P. A. Andrews, R. Brown, S. G. Chaney, A. Vaisman, D. Fink, S. B. Howell, M. S. Highley, A. H. Calvert, P. J. O'Dwyer, J. P. Stevenson, S. W. Johnson and M. J. Mckeage, in *Platinum Based Drugs in Cancer Therapy*, ed. R. Kelland and N. P. Farrell, Humana Press, Totowa, USA, 2000, pp. 3–35.
62 M. Watabe, M. Kai, K. Goto, H. Ohmuro, S. Furukawa, N. Chikaraishi, T. Takayama and Y. Koike, *J. Inorg. Biochem.*, 2003, **97**, 240.
63 M. El-Khateeb, T. G. Appleton, L. R. Gahan, B. G. Charles, S. J. Berners-Price and A.-M. Bolton, *J. Inorg. Biochem.*, 1999, **77**, 13.
64 M. E. Oehlsen, Y. Qu and N. Farrell, *Inorg. Chem.*, 2003, **42**, 5498.
65 S. J. S. Kerrison and P. J. Sadler, *Inorg. Chim. Acta*, 1985, **104**, 197.
66 T. V. O'Halloran and S. J. Lippard, *J. Am. Chem. Soc.*, 1983, **105**, 3341.
67 S. L. Hollis and S. J. Lippard, *J. Am. Chem. Soc.*, 1983, **105**, 3494.
68 I. R. Herbert, P. S. Pregosin and H. Rüegger, *Inorg. Chim. Acta*, 1986, **112**, 29.
69 T. V. O'Halloran, M. M. Roberts and S. J. Lippard, *Inorg. Chem.*, 1986, **25**, 957.
70 T. G. Appleton, J. R. Hall and D. W. Neale, *Inorg. Chim. Acta*, 1985, **104**, 19.
71 F. M. MacDonald and P. J. Sadler, ^{195}Pt NMR Spectroscopy: Applications to the study of anticancer drugs, in *Association for International Cancer Research and Symposia*, ed. D. C. H. McBrien and T. F. Slater, IRL Press, Oxford, UK, 1986, pp. 361–381.
72 M. Reithofer, M. Galanski, A. Roller and B. K. Keppler, *Eur. J. Inorg. Chem.*, 2006, 2612.
73 N. A. Bokach, A. V. Khripoun, V. Y. Kukushkin, M. Haukka and A. J. L. Pombeiro, *Inorg. Chem.*, 2003, **42**, 896.
74 M. Watabe, M. Kai, S. Asanuma, M. Yoshikane, A. Horiuchi, A. Ogasawara, T. Watanabe, T. Mikami and T. Matsumoto, *Inorg. Chem.*, 2001, **40**, 1496.
75 J. Autschbach and T. Ziegler, *J. Am. Chem. Soc.*, 2001, **123**, 5320.
76 T. G. Appleton, F. J. Pesch, M. Wienken, S. Menzer and B. Lippert, *Inorg. Chem.*, 1992, **31**, 4410.
77 S. Hintermann, P. S. Pregosin, H. Rüegger and H. C. Clark, *J. Organomet. Chem.*, 1992, **435**, 225.
78 A. Albinati, S. Caloupka, F. Demartin, T. F. Koetzle, H. Rüegger, L. M. Venanzi and M. K. Wolfer, *J. Am. Chem. Soc.*, 1993, **115**, 169.
79 B. P. Gracey, B. E. Mann and C. M. Spencer, *J. Organomet. Chem.*, 1985, **297**, 375.
80 K. Siegmann, P. S. Pregosin and L. M. Venanzi, *Organometallics*, 1989, **8**, 2659.
81 H. C. Clark, M. J. Hampden-Smith and H. Rüegger, *Organometallics*, 1988, **7**, 2085.
82 D. Carmona, R. Thouvenot, L. M. Venanzi, F. Bachechi and L. Zambonelli, *J. Organomet. Chem.*, 1983, **250**, 589.
83 A. Albinati, F. Lianza, H. Berger, P. S. Pregosin, H. Rüegger and R. W. Kunz, *Inorg. Chem.*, 1993, **32**, 478.
84 O. F. Wendt and L. I. Elding, *Inorg. Chem.*, 1997, **36**, 6028.
85 J. G. Kraaijkamp, D. M. Grove, G. van Koten and A. Schmidpeter, *Inorg. Chem.*, 1988, **27**, 2612.
86 I. Georgii, B. E. Mann, B. F. Taylor and A. Musco, *Inorg. Chim. Acta*, 1984, **86**, L81.
87 A. Musco, R. Pontellini, M. Grassi, A. Sironi, S. V. Meille, H. Rüegger, C. Ammann and P. S. Pregosin, *Organometallics*, 1988, **7**, 2130.
88 H. Rüegger and P. S. Pregosin, *Inorg. Chem.*, 1987, **26**, 2912.
89 C. Tessier and F. D. Rochon, *Inorg. Chim. Acta*, 2001, **322**, 37.
90 N. Nédélec and F. D. Rochon, *Inorg. Chim. Acta*, 2001, **319**, 95.
91 F. D. Rochon and C. Tessier, *Can. J. Chem.*, 2002, **80**, 379.
92 F. D. Rochon and V. Buculei, *Can. J. Chem.*, 2004, **82**, 524.
93 J. R. L. Priqueler, I. S. Butler and F. D. Rochon, *Appl. Spectrosc. Rev.*, 2006, **41**, 185 and references within.
94 A. Albinati, J. Eckert, P. S. Pregosin, H. Rüegger, R. Salzmann and C. Stössel, *Organometallics*, 1997, **16**, 579.
95 R. Romeo, L. M. Scolaro, N. Nastasi, B. E. Mann, G. Bruno and F. Nicolo, *Inorg. Chem.*, 1996, **35**, 7691.
96 A. Albinati, C. Arz and P. S. Pregosin, *Inorg. Chem.*, 1987, **26**, 508.
97 T. B. T. Ha, J. P. Souchard, F. L. Wimmer and N. P. Johnson, *Polyhedron*, 1990, **9**, 2647.
98 I. M. Ismail, S. J. S. Kerrison and P. J. Sadler, *Polyhedron*, 1982, **1**, 57.
99 P. G. A. Kumar, P. Dotta, R. Hermatschweiler, P. S. Pregosin, A. Albinati and S. Rizzato, *Organometallics*, 2005, **24**, 1306.
100 M. R. Plutino, S. Otto, A. Roodt and L. I. Elding, *Inorg. Chem.*, 1999, **38**, 1233.
101 F. D. Rochon and L. Fleurent, *Inorg. Chim. Acta*, 1988, **143**, 81.
102 F. D. Rochon and V. Buculei, *Inorg. Chim. Acta*, 2005, **358**, 3919.
103 T. G. Appleton, J. W. Connor, J. R. Hall and P. D. Prenzler, *Inorg. Chem.*, 1989, **28**, 2030.
104 R. E. Norman, J. D. Ranford and P. J. Sadler, *Inorg. Chem.*, 1992, **31**, 877.
105 T. G. Appleton, K. J. Barnham, J. R. Hall and M. T. Mathieson, *Inorg. Chem.*, 1991, **30**, 2751.
106 T. G. Appleton, J. R. Hall and I. J. McMahon, *Inorg. Chem.*, 1986, **25**, 720.
107 D. C. Caskey, R. K. Shoemaker and J. Michl, *Org. Lett.*, 2004, **6**, 2093.
108 J. J. Garcia, B. E. Mann, H. Adams, N. A. Bailey and P. M. Maitlis, *J. Am. Chem. Soc.*, 1995, **117**, 2179.
109 H. C. Clark, G. Ferguson, M. J. Hampden-Smith, B. Kaitner and H. Rüegger, *Polyhedron*, 1988, **7**, 1349.
110 S. J. Barton, K. J. Barnham, A. Habtemariam, R. E. Sue and P. J. Sadler, *Inorg. Chim. Acta*, 1998, **273**, 8.
111 D. Gudat, V. K. Jain, A. Klein, T. Schurr and S. Zalis, *Eur. J. Inorg. Chem.*, 2005, 4056.
112 B. Wrackmeyer, B. Ullmann, R. Kempe and M. Herberhold, *Z. Anorg. Allg. Chem.*, 2005, **631**, 2629.
113 S. Balters, E. Bernhardt, H. Willner and T. Berends, *Z. Anorg. Allg. Chem.*, 2004, **630**, 257.
114 F. Bachechi, G. Bracher, D. M. Grove, B. Kellenberger, P. S. Pregosin, L. M. Venanzi and L. Zambonelli, *Inorg. Chem.*, 1983, **22**, 1031.
115 T. G. Appleton, J. R. Hall, D. W. Neale and S. F. Ralph, *Inorg. Chim. Acta*, 1983, **77**, L149.

116 M. Mizuno, M. Suhara, T. Asaji and Y. Furukawa, *J. Mol. Struct.*, 1995, **345**, 123.
117 M. Itoh, M. Mori, M. Tanaka and H. Takei, *Physica B*, 1999, **259–261**, 999.
118 J. B. Robert and A. L. Barra, *Chirality*, 2001, **13**, 699.
119 M. Yogi, Y. Kitaoka, S. Hashimoto, T. Yasuda, R. Settai, T. D. Matsuda, Y. Haga, Y. Onuki, P. Rogl and E. Bauer, *Physica B (Amsterdam)*, 2005, **359–361**, 389.
120 D. Karshtedt, A. T. Bell and T. D. Tilley, *J. Am. Chem. Soc.*, 2005, **127**, 12640.
121 P. J. Martellaro, S. K. Hurst, R. Larson, E. H. Abbot and E. S. Peterson, *Inorg. Chim. Acta*, 2005, **358**, 3377.
122 S. U. Dunham and E. H. Abbot, *Inorg. Chim. Acta*, 2000, **297**, 72.
123 Ö. Gröning, T. Drakenberg and L. I. Elding, *Inorg. Chem.*, 1982, **21**, 1820.
124 Ö. Gröning and L. I. Elding, *Inorg. Chem.*, 1989, **28**, 3366.
125 G. Uccello-Barretta, R. Bernardini, F. Balzano and P. Salvadori, *Chirality*, 2002, **14**, 484.
126 G. Uccello-Barretta, R. Bernardini, F. Balzano and P. Salvadori, *J. Org. Chem.*, 2001, **66**, 123.
127 F. M. Macdonald and P. J. Sadler, *Polyhedron*, 1991, **10**, 1443.
128 S. J. S. Kerrison and P. J. Sadler, *Inorg. Chim. Acta*, 1985, **104**, 197.
129 A. Klein, T. Schurr, A. Knoedler, D. Gudat, K. W. Klinkhammer, V. K. Jain, S. Zalis and W. Kaim, *Organometallics*, 2005, **24**, 4125.
130 N. V. Kaminskaia, G. M. Ullmann, D. B. Fulton and N. M. Kostic, *Inorg. Chem.*, 2000, **39**, 5004.
131 E. T. Martins, H. Baruah, J. Kramarczyk, G. Saluta, C. S. Day, G. L. Kucera and U. Bierbach, *J. Med. Chem.*, 2001, **44**, 4492.
132 N. J. Wheate, L. K. Webster, C. R. Brodie and J. G. Collins, *Anti-Cancer Drug Des.*, 2000, **15**, 313.
133 N. J. Wheate and J. G. Collins, *J. Inorg. Biochem.*, 2000, **78**, 313.
134 N. J. Wheate, B. J. Evison, A. J. Herlt, D. R. Phillips and J. G. Collins, *Dalton Trans.*, 2003, 3486.
135 N. J. Wheate, D. P. Buck, A. I. Day and J. G. Collins, *Dalton Trans.*, 2006, 451.
136 B. N. Shelimov, J. F. Lambert, M. Che and B. Didillon, *J. Mol. Catal. A: Chem.*, 2000, **158**, 91.
137 P. J. Pellechia, J. X. Gao, Y. L. Gu, H. J. Ploehn and C. J. Murphy, *Inorg. Chem.*, 2004, **43**, 1421.
138 Z. Beni, R. Scopelliti and R. Roulet, *Inorg. Chem. Commun.*, 2004, **7**, 935.
139 E. W. Abel, I. Moss, K. G. Orrell, V. Sik and D. Stephenson, *J. Chem. Soc., Dalton Trans.*, 1987, 2695.
140 P. K. Babu, H. S. Kim, J. H. Kuk, J. H. Chung, E. Oldfiled, A. Wieckowski and E. S. Smotkins, *J. Phys. Chem. B*, 2005, **109**, 17192.
141 H. Tou, K. Ishida and Y. Kitaoka, *Physica C (Amsterdam)*, 2004, **408–410**, 305.
142 G. Ma, M. Maliarik, L. Sun and J. Glaser, *Inorg. Chim. Acta*, 2004, 4073.
143 T. G. Appleton, *Coord. Chem. Rev.*, 1997, **166**, 313.
144 T. Peleg-Shulman, Y. Najajreh and D. Gibson, *J. Inorg. Biochem.*, 2002, **91**, 306.
145 L. Szucova, T. Zdenek, M. Zatloukal and I. Popa, *Bioorg. Med. Chem.*, 2006, **14**, 479.
146 L. Wu, B. E. Schwederski and D. W. Margerum, *Inorg. Chem.*, 1990, **29**, 3578.
147 T. G. Appleton, J. R. Hall, S. F. Ralph and C. S. M. Thompson, *Inorg. Chem.*, 1989, **28**, 1989.
148 S. J. Berners-Price and P. W. Kuchel, *J. Inorg. Biochem.*, 1990, **38**, 305.
149 J. K. Barton and S. J. Lippard, Metal Ions in Biology, in *Nucleic Acid–Metal Ion Interactions*, ed. T. G. Spiro, John Wiley, New York, USA, 1980.
150 S. J. Berners-Price, U. Frey, J. D. Ranford and P. J. Sadler, *J. Am. Chem. Soc.*, 1993, **115**, 8649.
151 I. M. Ismail and P. J. Sadler, *J. Inorg. Biochem.*, 1984, **22**, 103.
152 G. M. Clore and A. M. Gronenborn, *J. Am. Chem. Soc.*, 1982, **104**, 1369.
153 B. A. J. Jansen, J. M. Perez, A. Pizarro, C. Alonso, J. Reedijk and C. Navarro-Ranninger, *J. Inorg. Biochem.*, 2001, **85**, 229.
154 A. A. Tulub and V. E. Stefanov, *Int. J. Biol. Macromol.*, 2001, **28**, 191.
155 T. G. Appleton, J. R. Hall and S. F. Ralph, *Inorg. Chem.*, 1985, **24**, 673.
156 M. Becker, R. E. Port, H.-J. Zabel, W. J. Zeller and P. Bachert, *J. Magn. Reson.*, 1998, **133**, 115.
157 M. S. Ali, S. R. A. Khan, H. Ojima, I. Y. Guzman, K. H. Whitmire, Z. H. Siddik and A. R. Khokhar, *J. Inorg. Biochem.*, 2005, **99**, 795.
158 S. Kemp, N. J. Wheate, S. Wang, J. G. Collins, A. I. Day, V. J. Higgins and J. R. Aldrich-Wright, *Unpublished Results*, 2006.
159 S. Kemp, *Unpublished Results*, 2006.
160 W. S. Price, *Concepts Magn. Reson.*, 1997, **9**, 299.
161 P. S. Pregosin, P. G. A. Kumar and I. Fernandez, *Chem. Rev.*, 2005, **105**, 2977.
162 R. Siegel, T. T. Nakashima and R. E. Wasylishen, *J. Phys. Chem. B*, 2004, **108**, 2218.
163 A. Grykalowska and B. Nowak, *Solid State Nuclear Magn. Reson.*, 2005, **27**, 223.
164 A. A. Lysova, I. V. Koptyug, R. Z. Sagdeev, V. N. Parmon, J. A. Bergwerff and B. M. Weckhuysen, *J. Am. Chem. Soc.*, 2005, **127**, 11916.

